Off-center phonon scattering sites in $Eu_8Ga_{16}Ge_{30}$ and $Sr_8Ga_{16}Ge_{30}$

R. Baumbach,[1] F. Bridges,[1] L. Downward,[1] D. Cao,[1] P. Chesler,[1] and B. Sales[2]
[1]*Physics Department, University of California, Santa Cruz, California 95064, USA*
[2]*Oak Ridge National Laboratory, Oak Ridge, Tennessee 37831-6393, USA*
(Received 7 July 2004; revised manuscript received 18 October 2004; published 20 January 2005)

We present a detailed extended x-ray absorption fine structure (EXAFS) analysis of the thermoelectric clathrates $Eu_8Ga_{16}Ge_{30}$ and $Sr_8Ga_{16}Ge_{30}$, both of which have an unusually low thermal conductivity attributed to a "rattler" motion of the filler atoms Eu and Sr. The EXAFS results show that the Ga/Ge lattice is quite stiff with a high correlated Debye temperature ~400 K. Eu is on-center in the site 1 cage but off-center (0.445 ± 0.020 Å) in the large cage called the Eu2 site. The results for Sr are similar, but ~75% are off-center 0.40 ± 0.05 Å and ~25% are on-center in the Sr2 site. Both results are in reasonable agreement with diffraction results. The temperature dependence of the nearest neighbor pair distribution widths yield low Einstein temperatures (80 ± 10 and 100 ± 10 K for Eu1 and Sr1, respectively, and 95 ± 10 and 125 ± 10 K for the shortest Eu2-Ga/Ge and Sr2-Ga/Ge pairs). In contrast, the more distant Eu2/Sr2-Ga/Ge pair distributions within the Eu2/Sr2 cage are strongly disordered even at low *T*, indicating considerable local disorder. This indicates that the off-center Eu or Sr atom is bonded to the side of the site 2 cage. This has two important implications for the thermal conductivity: it increases the coupling between the "rattler" vibrations and the lattice phonons and it introduces a symmetry-breaking large mass defect.

DOI: 10.1103/PhysRevB.71.024202 PACS number(s): 72.20.Pa, 61.10.Ht, 66.70.+f

I. INTRODUCTION

Recently, a number of materials with open crystal structures, such as the skutterudites and some filled clathrates, have attracted attention because of their potential as thermoelectrics. When voids in these structures are filled with another type of atom (e.g., Ce, Eu, Sr), the thermal conductivity, κ, is greatly reduced and can approach that of a glass. A low value of κ is a prerequisite for improving the figure of merit ZT for a thermoelectric (defined as $ZT = TS^2\sigma_e/\kappa$), where *S* is the Seebeck coefficient, *T* is temperature, and σ_e is the electrical conductivity.[1–3] Some existing thermoelectrics can have ZT close to 1—a goal is to increase ZT by a factor of 3 or more. To do so we need a better understanding of these materials on a fundamental level. Slack[4] introduced the idea of an electron-crystal/phonon-glass to describe the high electrical and low thermal conductivity characteristics of an ideal thermoelectric material. For these open crystal structures, the main lattice-framework provides the high electrical conductivity (often semiconductor-like) while the low thermal conductivity is attributed to the scattering of phonons by the filler atom located within "cages" of the structure. The addition of filler atoms changes the properties considerably.[5–8]

For the filled type-I clathrates (e.g., $Eu_8Ga_{16}Ge_{30}$) the ideal material should be an intrinsic semiconductor; each Ga is defficient by one electron (16 per formula unit) while Eu and other +2 filler ions provide two electrons (again 16 per formula unit); if the compound is stoichiometric and the distribution of atoms homogeneous, there is no net doping. An alternative way to view this Zintl material is as a highly compensated semiconductor. The filler atoms are donors—they donate electrons to the Ga/Ge framework and the filler atom is expected to have a net positive charge. Ga atoms in Ge form *p*-type donors—and if *p*-type carriers become delocalized, then Ga should have a net negative charge.

However, the actual charge on the rattler atom has been a recent question of debate. Although experimental papers treat Sr, Ba, and Eu as +2 ions,[9,10] early calculations of the Sr clathrate suggested that Sr was essentially neutral[11]—and an x-ray absorption near-edge structure (XANES) paper appeared to agree.[12] More recent calculations by Gatti *et al.*[13] indicate that Sr and Ba in these clathrates are largely ionic, but the partioning of charge in their model is based on quantum mechanics and not geometric considerations. In addition, XANES might not be a good way to probe the valence issue for many semiconducting/Zintl materials. We have carried out extended x-ray absorption fine structure (EXAFS) experiments on a large number of skutterudites of the form LT_4X_{12} (L=Ce,Eu,Yb; T=Fe,Ru,Os; X=P,Sb);[14–16] XANES studies on the same samples show that for Fe, Ru, Os, and Sb, the absorption edge in the skutterudite sample overlaps that of the elemental metal very well.[17] A resolution of the discrepancy between Zintl and more ionic materials is outside the scope of this paper but may depend on similar arguments to those of Gatti *et al.*[13]

A more important question that has not really been addressed is the effective charge on the Ga atoms. Gatti *et al.*[13] argue that the rattler-cage interaction must be electrostatic because of the electron charge transfer from the rattler atom to the Ga/Ge framework, but they do not discuss variations of electron density on the Ga and Ge atoms. If the electrons are highly delocalized one might treat the cage as having a uniform negative charge; however, if the Ga are partially negative then the rattler will be more attracted to them and that would determine the strongest bonds. We return to this possibility in the Discussion section.

A complication to the above ideas is that for most investigations of filled-clathrate materials, defects and nonstoichiometry usually result in *n*-type semiconducting behavior. For

such *n*-type materials, a low thermal conductivity has been observed[9,10] with filler atoms Ba, Sr, or Eu, which occupy two cages in the clathrate structure, referred to as sites 1 and 2.[10,18] In these materials all three atoms have large thermal parameters in diffraction studies (but much larger for Eu and Sr). The temperature dependence indicates that these atoms vibrate with low energies; consequently they fit the description of "rattler" atoms. It is well known that such oscillators can resonantly scatter phonons for phonon frequencies near the vibration frequency of the "rattler."[1] However, for *n*-type $Ba_8Ga_{16}Ge_{30}$, the temperature dependence of the thermal conductivity is more like that of a crystal [i.e., $\kappa(T)$ has a peak at low T, near 20 K][10] while the Eu and Sr versions are more glasslike with a plateau region above 200–250 K and a decreasing thermal conductivity at lower T, with another small dip/plateau region near 20–30 K.[9,10] In addition, the magnitude of the thermal conductivity for a given filler atom (in *n*-type materials) varies considerably between samples at low T.[9,10,19,20]

The difference between the behavior for the Ba and the Eu/Sr *n*-type systems is not well understood—but appears to be related to Eu and likely Sr having a large off-center displacement[9,10,21–23] in the Eu2 and Sr2 sites, while Ba2 is on-center.[10] For the off-center case, there are then several equivalent off-center positions (here 4) and in general the off-center atom (Eu and Sr) can tunnel between equivalent sites, as is well known for off-center systems in the alkali halides. For heavy off-center defects such as Ag and Cu, the tunneling[24,25] is very slow (<20 GHz) compared to phonon frequencies and therefore the tunneling states should only scatter phonons at low T, $\leqslant 1$ K. The tunneling frequencies have not yet been determined in the clathrates (an upper limit, $\ll 1$ K, has recently been determined[26]) but little else is known about them.

Very recently, *p*-type single crystal material has been prepared by growing the crystal in a Ga-rich environment. For *p*-type $Ba_8Ga_{16}Ge_{30}$, the thermal conductivity is greatly reduced and has a slight dip/plateau region near 20 K, similar to that for the Eu and Sr systems.[19] Unfortunately there is, as of yet, no structural information about this *p*-type material, particularly as to whether the Ba is, or is not, displaced off-center within site 2. Bentien *et al.*[19] note that there is an unusually wide range in the thermal conductivity reported for $Ba_8Ga_{16}Ge_{30}$ at low T; $\kappa(T)$ is quite high for some *n*-type materials and nearly two orders of magnitude lower for the *p*-type material at 10 K.[10,19,20] Although Sales *et al.*[10] find Ba on-center in their single crystal samples, Bentien *et al.*[19] question that result and instead suggest that the wide variation in the properties of the filled clathrates at low T is primarily the result of changes in phonon/charge-carrier scattering; however, they do not explain why two *n*-type samples of nearly the same carrier concentration and effective mass can have carrier scattering lengths that vary by an order of magnitude. Until detailed structural measurements for a range of Ba samples are available, this issue cannot be resolved.

In this paper, we present a detailed local structure study of *n*-type $Eu_8Ga_{16}Ga_{30}$ and $Sr_8Ga_{16}Ga_{30}$ to address several issues. First, using EXAFS, the off-center displacement can be directly measured and the Einstein frequency determined for the (radial) rattler mode vibration of Eu2 or Sr2 toward the nearest neighbor Ga/Ge. This is different from the isotropic thermal parameters for Eu and Sr measured in diffraction. Assuming the tunneling frequencies are of the same order as observed in the alkali halides, the tunneling will be slow and quasistatic from the perspective of the phonons, and an off-center Eu2 or Sr2 will form a bond to the nearest Ga/Ge atoms—we show that the PDF for this short bond is well defined, with a fairly low static broadening and a temperature dependent width, well described by a correlated Einstein model. The resulting correlated Einstein temperatures θ_E are larger than the lowest value reported in diffraction (an isotropic average) but agree quite well with peaks in the Raman spectra.

We argue that the off-center rattlers produce two effects of importance for lowering the thermal conductivity of thermoelectric materials: (1) the off-center atom is bound to the nearest Ga/Ge atoms in the cage and hence its local mode vibrations are more strongly coupled to the phonons of the Ga/Ge lattice than for an on-center atom, and (2) the random occupation of the four off-center positions by the heavy Eu or Sr atoms produces a symmetry-breaking heavy mass defect that should scatter intermediate phonon wavelengths effectively.

The outline of the paper is as follows: in Sec. II we provide some of the experimental details about the samples and the EXAFS technique. The data are presented in Sec. III, and the detailed fits, including the constraints used, are described in Secs. IV and V. The results are discussed and compared with other measurements in Sec. VI, which also includes a discussion of the implications for thermal conductivity. The conclusions are summarized in Sec. VII.

Background: Clathrate structure

The clathrate crystal structure (space group $Pm3n$) is composed of two polyhedral groups (cages) made up of 34.78% Ga and 65.21% Ge (i.e., a 16:30 ratio in the stoichimetric compound). Each of the cages encloses a Eu/Sr atom. The first (smaller) cage, referred to as the Eu1/Sr1 site, contains 20 Ga/Ge atoms and holds 25% of the Eu/Sr. For this site, the Eu/Sr atom remains on-center. The more numerous Eu2/Sr2 cage (75% of the Eu/Sr), shown in Fig. 1, contains 24 Ga/Ge atoms and is formed of three types of crystallographic sites [M1(6*c*), M2(16*i*), and M3(24*k*)].[18,27] This cage is proposed to house a rattler atom (Eu or Sr).

Neutron diffraction studies on *n*-type material suggest that the Eu2/Sr2 rattlers are displaced off-center to one of two Wyckoff sites, 24*k* or 24*j*. 24*k* is equivalent to Eu2 being displaced along the $\pm\hat{b}$ or $\pm\hat{c}$ axes, see Fig. 1. We call this a $(0,0,\Delta)$ or $(0,\Delta,0)$ displacement. The 24*j* displacement model has the Eu2 displaced equally along the $\hat{b}$ and $\hat{c}$ axes, toward the midpoint between two M2 sites (Fig. 1). This is called a $(0,\Delta,\Delta)$ displacement. The magnitudes of the displacement Δ from neutron diffraction are $\sim$0.4 and $\sim$0.3 Å for $Eu_8Ga_{16}Ge_{30}$ and $Sr_8Ga_{16}Ge_{30}$, respectively.[18,27]

In addition, the neutron diffraction thermal ellipses also show significant broadening along the $\hat{a}$ axis; consequently a small displacement along the $\hat{a}$ axis is also possible. Adding a small $\hat{a}$ component leads to a modified 24*k* displacement

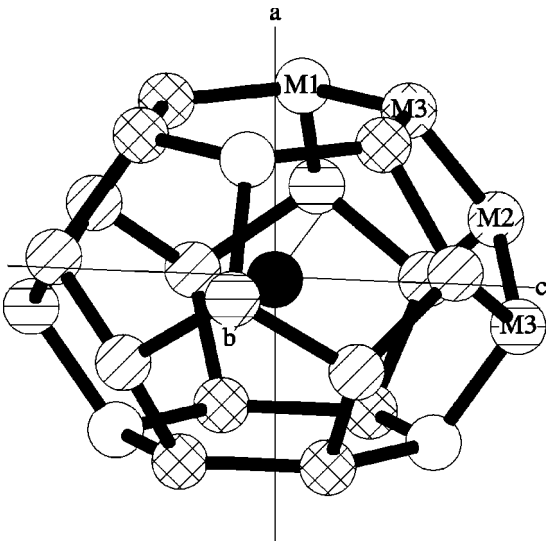

FIG. 1. The Eu2/Sr2 cage showing the M-sites (from Refs. 18 and 27); M1 site—white; M2 site—diagonal lines; near M3 site—diagonal crosshatch; distant M3 site—horizontal lines.

model, $(\delta,\Delta,0)$, discussed in detail in Sec. IV A. The reason we consider other models is that the forces that move the atom off-center are determined by the minima in the local potential, which are dominated by a few nearest neighbors assuming the interactions with the nearest neighbors are essentially equivalent.

II. EXPERIMENTAL DETAILS

A. Samples

The sample preparation has been reported earlier.[10] The Sr material is identical to that investigated in Ref. 27 while the Eu version is prepared the same way as the samples studied in Ref. 18. For the EXAFS samples, a small amount of single crystal material was ground and then passed through a 400-mesh sieve. Next, the resulting fine powder was spread onto Scotch tape using a fine brush. In this process the larger of the fine particles were removed; typical remaining particle size is $<10\ \mu$. Several layers of tape were then stacked to make samples with an absorption step height between 0.3 and 1 for the different edges.

B. XAFS technique

The experimental EXAFS function χ is obtained from the absorption data using the equation $\chi=(\mu-\mu_0)/\mu_0$, where μ is the absorption coefficient for the edge (pre-edge background removed) and μ_0 is the background (embedded atom) function.[28]

The EXAFS equation we use in analyzing the data is

$$k\chi(k)=\sum_i k\chi_i(k)=\mathrm{Im}\sum_i kA_i e^{2/3k^4C_{4i}}e^{i[2\delta_c(k)+\delta_i(k)-4/3k^3C_{3i}]}\times\int_0^\infty F_i(k,r)\frac{g_i(r_{0i},r)e^{i2kr}}{r^2}dr, \quad (1)$$

where χ_i is the XAFS function for shell i, $F_i(k)$ is the backscattering amplitude of the photoelectron from neighbors i (it includes mean-free path effects), and $g_i(r_{0i},r)$ is the (Gaussian) pair distribution function for the atoms at a distance r_{0i}. The phase shifts, $\delta_c(k)$ and $\delta_i(k)$, correspond to the central and backscattering atom potentials, respectively. The amplitude A_i is defined by $A_i=N_iS_0^2$ where N_i is the coordination number of shell i and S_0^2 is the amplitude reduction factor that arises from many-body effects and small corrections to the effective mean-free path in the theoretical functions. The parameters C_3 and C_4 describe the asymmetry and the kurtosis of the PDF and usually can be neglected unless the k-range is very long. Finally, the photoelectron wave vector k is defined by $k=\sqrt{2m_e(E-E_0)/\hbar^2}$, where E_0 is the binding energy for the absorption edge under study.

III. XAFS DATA

XAFS data were collected as a function of temperature at the Stanford Synchrotron Radiation Laboratory (SSRL) for the Sr, Ga, and Ge K-edges, and the Eu L_{III}-edge of $Eu_8Ga_{16}Ge_{30}$ and $Sr_8Ga_{16}Ge_{30}$. The measurements were carried out on beamline 4-3 using Si 220 monochromator crystals. The monochromator was detuned 50% to reduce harmonics; the slit height was 0.7 mm for all edges, giving energy resolutions of 0.5, 1.3, 1.3, and 2.8 eV for the Eu L_{III} and Ga, Ge, and Sr K-edges, respectively. At each temperature, the sample position was reset (because of thermal expansion/contraction of the probe) so that the region of the sample studied remained the same (within $\sim 50\ \mu$). The data were reduced using standard procedures[29–31] to yield XAFS oscillations as a function of k.

A. Eu L_{III}- and Sr K-edges

Plots of the Eu k-space and r-space data at low, mid, and high temperature are shown in Figs. 2(a) and 2(b). Figure 2(a) shows the high quality of the Eu k-space data from 3.00 to 11.00 Å^{-1}. The amplitude at high k decreases rapidly with increasing temperature and above 11.00 Å^{-1} little XAFS signal remains for much of the temperature range. Consequently, we used a k-range of 3.50 to 10.50 Å^{-1} for the Fourier transform (FT) to generate the r-space data; examples are shown in Fig. 2(b). The Sr k-space data are shown in Fig. 3(a). Again the amplitude at high k decreases rapidly with T; here we used a k-space range of 3.50 to 11.50 Å^{-1} to generate the FTs. Some examples of the Sr r-space data are shown in Fig. 3(b).

Within the two cage structures there are several different Eu/Sr-Ga/Ge distances (see Table I) ranging from 3.4 to 4.5 Å. A peak in the XAFS r-space data is always shifted slightly to lower r, typically by 0.3 Å, because of a well known phase factor. For both the Sr and Eu edges the sum of the peaks near $\sim$3.15 Å in Figs. 2(b) and 3(b) (corresponding to distances near 3.5 Å) is large at low temperatures indicating little disorder (small broadening) for the shorter Eu/Sr-Ga/Ge nearest neighbor distances. The amplitude of this peak which has contributions from both cages is strongly temperature dependent, decreasing by $\sim$75% between 15 and 310 K. This implies that the shorter Eu/Sr

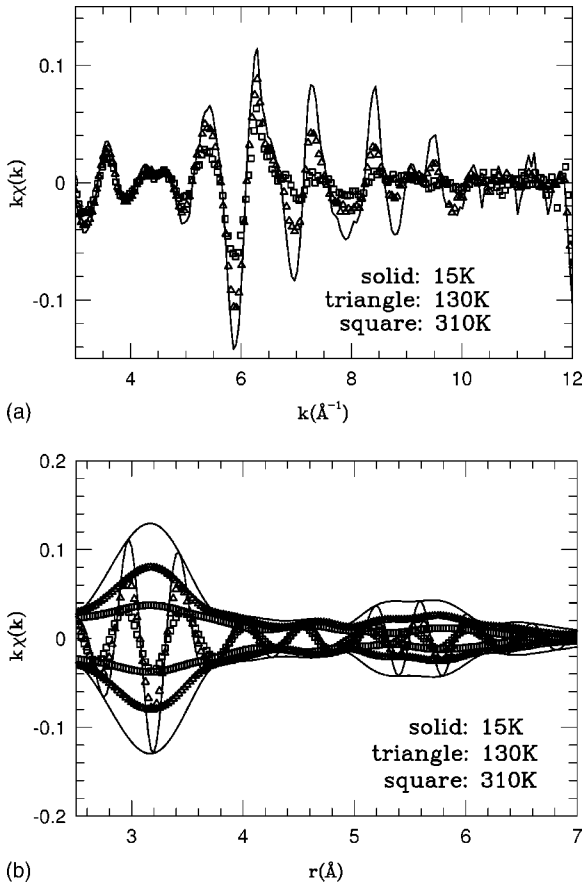

FIG. 2. (a) The Eu L_{III}-edge *k*-space data for three different temperatures. (b) The Fourier transform of the data in (a) for a transform range of 3.50–10.50 Å^{-1}, with a 0.3 Å^{-1} Gaussian broadening. In this and other Fourier transform (FT) plots, the envelope is defined as $\pm\sqrt{\mathrm{FT}_R^2+\mathrm{FT}_I^2}$, where FT_I is the imaginary part and FT_R the real part of the FT. The high frequency curve inside the envelope is FT_R. The first peak (~3–4.4 Å) represents the shell of neighboring atoms (the cages) surrounding the central Eu atom while the second and third peaks (above 5 Å) represent more distant Ga/Ge neighbors outside these cages.

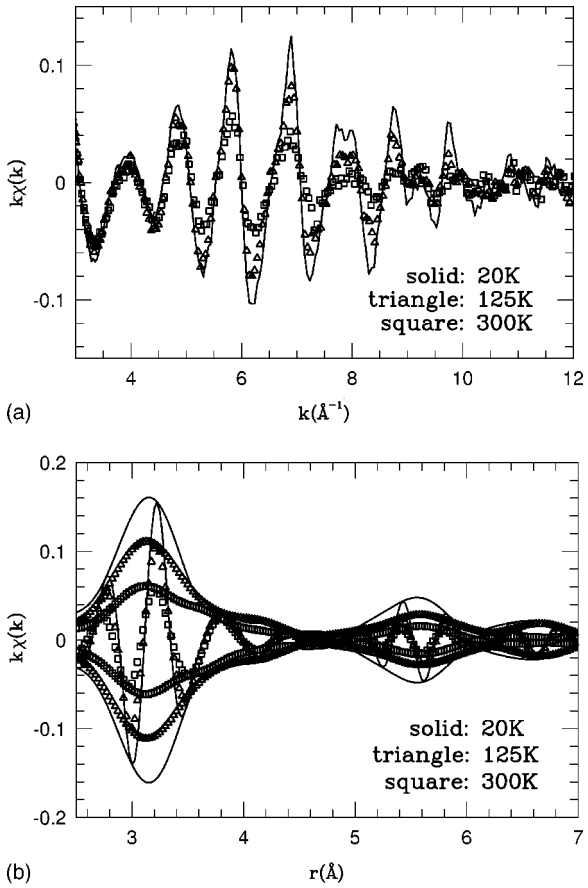

FIG. 3. (a) The Sr *K*-edge *k*-space data for three different temperatures. (b) The Fourier transform over a *k*-range of 3.50–11.50 Å^{-1}, with a 0.3 Å^{-1} Gaussian broadening. Here again the first peak represents the nearest neighbor shell of atoms (the cages) surrounding the central Sr atom while the second and third peaks represent Ga/Ge neighbors outside these cages.

-Ga/Ge pairs are connected by relatively weak springs compared to the stiffness of the Ga/Ge structure (see Sec. V C.

In contrast, the amplitude of the sum of the peaks in the 3.5–4.4 Å range is very low and shows little temperature dependence. The peaks that contribute in this range correspond to the longer Sr/Eu-Ga/Ge distances within the Sr2/Eu2 cages. The small amplitude at low *T* implies that a large amount of static disorder is present for these Eu/Sr -Ga/Ge pairs; the vibrational motions of these more distant Ga/Ge neighbors relative to Eu2/Sr2 may also be uncorrelated or possibly negatively correlated.

The peak between 5.00 and 6.00 Å also shows a strong temperature dependence, indicating that the longer Eu/Sr -Ga/Ge pair-distances are ordered at low *T* but become partially thermally disordered at 300 K. This peak corresponds to distances outside of the Ga/Ge cage immediately surrounding the Eu/Sr.

It is also interesting that with the exception of a phase change of the real part of the FT (FT_R), the shapes of the Eu and Sr *r*-space data are similar. This reflects their similar local structure.

B. FEFF7 simulations for Eu/Sr

Further understanding can be developed by first simulating the XAFS data using a sum of theoretical EXAFS functions (standards), *without any fits* to the experimental data. These are calculated using the computer program FEFF7[32] (developed by Rehr and co-workers), which calculates the theoretical XAFS functions χ_i, defined in Sec. II B.

Theoretical EXAFS standards were generated for the Eu1/Sr1 on-center sites and the Eu2/Sr2 $(0,0,\Delta)$, $(\delta,\Delta,0)$, and $(0,\Delta,\Delta)$ off-center models. Of the 20 Ga/Ge atoms surrounding an Eu1/Sr1, eight are at a distance of 3.41 Å and 12 are at ~3.52 Å. The site 2 cage contains 24 Ga/Ge, but since the central Eu2/Sr2 is off-center, the positions and degeneracies of these standards are more complex and depend on the magnitude of the displacement. They are discussed in more detail in Sec. IV A.

In Figs. 4(a) and 4(b) the simulations for the Eu1/Sr1 site are shown assuming the same broadening of each of the cage-neighbor pair distribution functions. For realistic values

TABLE I. Examples of nearest neighbor distances (in Å) from Eu/Sr to Ga/Ge when Sr2 is displaced 0.35 Å and Eu2, 0.45 Å.

Sr1	Sr2$(0,0,\Delta)$	Sr2$(\delta,\Delta,0)$	Eu1	Eu2$(0,0,\Delta)$	Eu2$(\delta,\Delta,0)$
3.4094	3.4019	3.4415	3.4005	3.3443	3.3959
3.5242	3.4827	3.4444	3.5253	3.4492	3.3998
	3.5435	3.5030		3.4688	3.4158
	3.6821	3.6865		3.5898	3.6041
	3.7250	3.6928		3.6940	3.6828
	3.7985	3.7959		3.7601	3.7112
	3.7989	3.8043		3.7622	3.7499
	3.8045	3.8366		3.7992	3.8481
	3.8139	3.8366		3.8537	3.9020
	4.0374	4.0019		4.1030	4.0583
	4.1596	4.1507		4.1625	4.1736
	4.1648	4.1733		4.2058	4.1947
	4.2767	4.2860		4.3538	4.3656
	4.4963	4.4890		4.5834	4.5744

of σ the amplitude of the Eu1/Sr1 standard at 3.10 Å is not large enough to model the experimental data. Therefore the Eu2/Sr2 sites must also contribute at this distance.

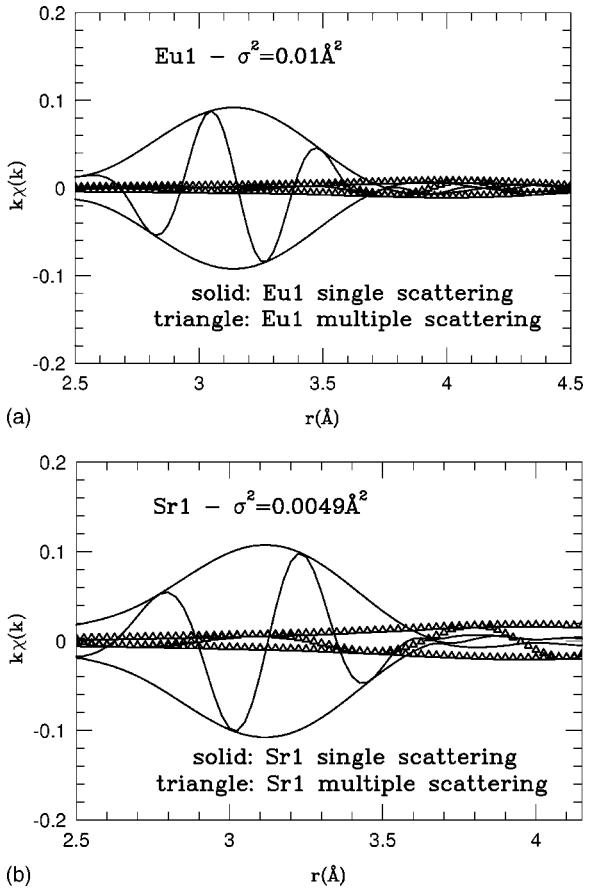

FIG. 4. (a) The Eu1 single and multiple scattering FEFF7 standards with a uniform broadening of σ=0.10 Å. (b) The Sr1 single and multiple scattering standards with σ=0.07 Å.

Similarly, Figs. 5(a), 5(b), 6(a), and 6(b) show uniformly broadened standards (σ=0.10 Å) for the $(0,0,\Delta)$ and $(\delta,\Delta,0)$ models at various Eu2/Sr2 off-center positions. The $(0,\Delta,\Delta)$ standards are not shown because they were found to be poor models for the data. For a significant off-center displacement, the Eu2/Sr2-Ga/Ge standards have considerable amplitude in the 3.0–3.2 Å region (with σ=0.10 Å) and make up for the missing amplitude that would arise if one attempted to model this range of distances using only the Eu1/Sr1 site. Also note the changing phase shift of FT_R as the off-center displacement increases from 0.0 to 0.3 Å. Consequently, when combined with the Eu1/Sr1 contribution, the phase of the resultant is shifted slightly in opposite directions (near 3.15 Å) for off-center displacements of 0.0 and 0.3 Å (see Figs. 5 and 6). Only for the off-center case does the phase (and the amplitude) of the resultant agree with the data. This is direct evidence of the necessity for Eu2/Sr2 to be off-center.

However, the overall shape of this uniformly broadened simulation for the Eu2 site does not describe the experimental data well over the entire range from 3 to 4.4 Å. In contrast to the results for the short distances, the simulations for the longer Eu/Sr-Ga/Ge distances (3.6–4.4 Å) must be broadened significantly ($\sigma\sim$0.20 Å) to match the amplitude of the data. This suggests that there is a large static disorder and/or the vibrations are uncorrelated for the longer Eu-Ga/Ge and Sr-Ga/Ge pair-distances in the Eu2/Sr2 cage.

It also should be noted that the FEFF7 calculations yield a non-negligible Eu1/Sr1 multiple scattering contribution between 3.00 and 4.20 Å (see Fig. 4) that must be included in the detailed fits.

C. Ga/Ge XAFS data

Plots of the Ga and Ge *r*-space data (*K*-edge) for the $Eu_8Ga_{16}Ge_{30}$ and $Sr_8Ga_{16}Ge_{30}$ samples are shown in Figs. 7(a), 7(b), 8(a), and 8(b) for three different temperatures. For

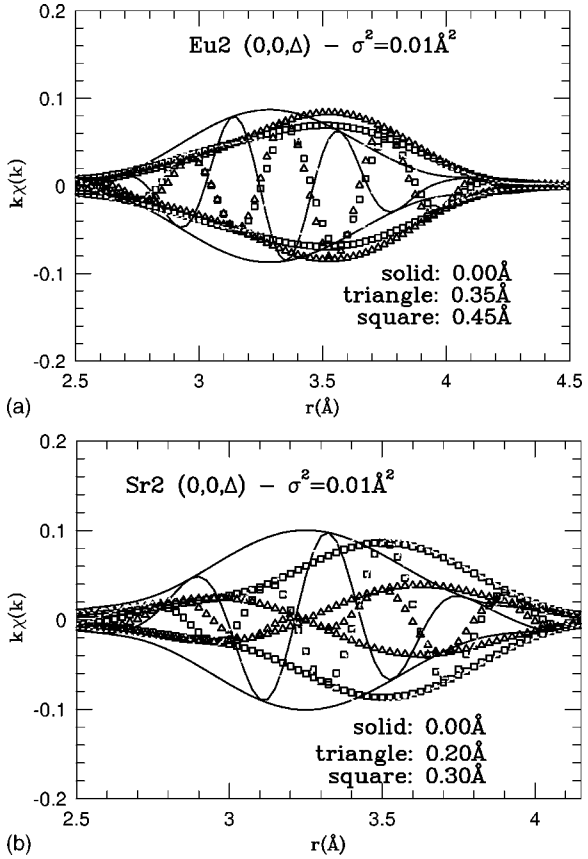

FIG. 5. (a) A sum of the Eu2 FEFF7 standards for the $(0,0,\Delta)$ model using off-center displacements 0.00, 0.35, and 0.45 Å. (b) A similar sum for Sr2 using off-center displacements of 0.00, 0.20, and 0.30 Å.

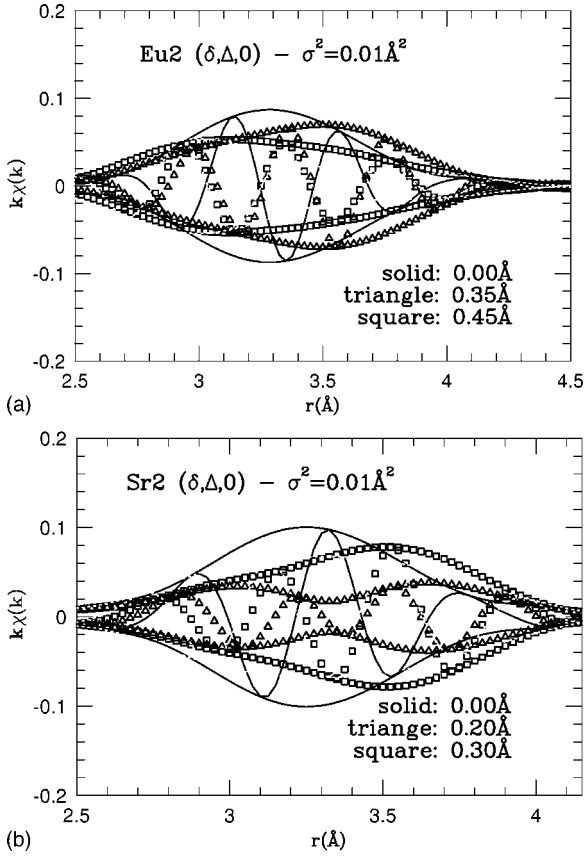

FIG. 6. (a) A sum of the Eu2 FEFF7 standards for the $(\delta,\Delta,0)$ model (σ=0.1 Å) using off-center displacements of 0.00, 0.35, and 0.45 Å. (b) The same sum for Sr2 using off-center displacements of 0.00, 0.20, and 0.30 Å.

both samples, the data looks almost identical for each edge. This is expected since Ga and Ge are neighbors in the periodic table (Z=31 and 32). Also, because the data look identical for both samples, it shows that the type of rattler atom has little effect on the behavior of the Ga/Ge cages.

The first two peaks in these plots occur at ~2.10 and 3.66 Å and correspond to the two shortest Ga/Ge-Ga/Ge distances in the structure. The weak temperature dependence of the first peak implies that the bonds between the nearest neighbor Ga/Ge atoms are stiff while the stronger temperature dependence for the second peaks shows that the effective spring constant between second neighbor Ga/Ge atoms is softer. This is not unexpected because small changes in the bond angles would produce significant changes in the second neighbor distances even if the bond lengths were constant.

Additionally, a very small peak (near 3.0 Å in Figs. 7 and 8) should correspond to the Ga/Ge-Eu/Sr distances. However, no obvious peak is present at this distance—it is severely broadened—and is not included in the fits.

IV. DETAILED FITTING PROCEDURES AND CONSTRAINTS

The general fitting procedures are similar for each edge. Appropriate FEFF7 functions are first calculated for each peak as described above for the simulations and then summed together with variable parameters to mimic the data using a program called RSFIT[31] (formerly called FIT); this program fits in r-space. However, each local environment will require a different set of constraints. In general there can be six parameters varied for each peak [see Eq. (1)]: the amplitude NS_o^2, the atom-pair distance r, the width of the pair-distribution function σ, the asymmetry parameter C_3, the kurtosis parameter C_4, and small changes in the edge energy, ΔE_o which determine where k=0 occurs for the photoelectron. Usually C_3 and C_4 have little influence on the XAFS k-space data until k is quite large; consequently when the FT range is short, as is the case here, they can often be neglected. Although some asymmetry (C_3) might be expected for the off-center sites at high T, there are not enough free parameters to obtain a unique fit including the C_3 parameter because of the complicated clathrate structure. Thus we will not discuss the C_3 and C_4 parameters further for this system.

The amplitude parameter NS_o^2 is determined at low T. Since we know the coordination number N from diffraction data, this is a measure of the parameter S_o^2 which describes many body effects. This parameter is then kept constant for fits at higher temperatures to minimize the effect of the correlations between the amplitude and the width σ.

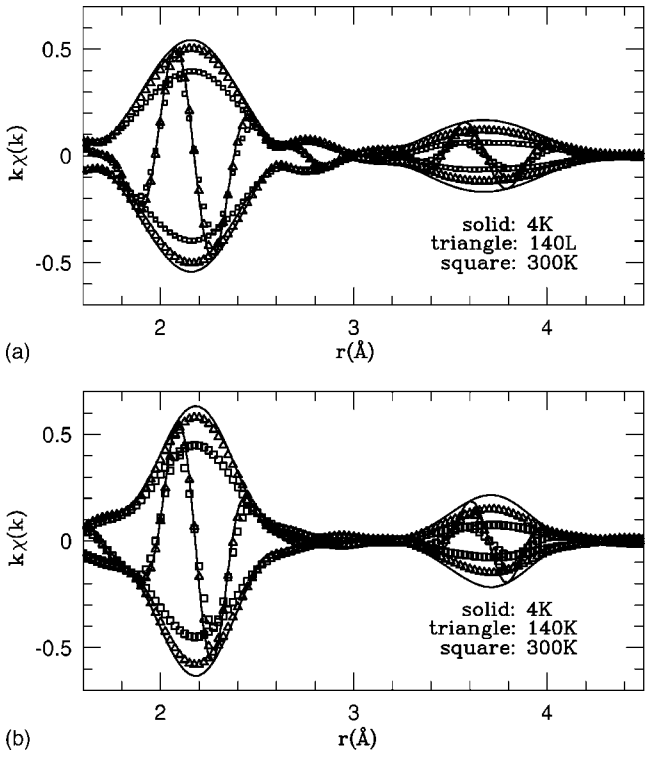

FIG. 7. (a) The Ga *K*-edge *r*-space data for $Eu_8Ga_{16}Ge_{30}$ at three different temperatures. (b): The Ge *K*-edge *r*-space data for the same sample.

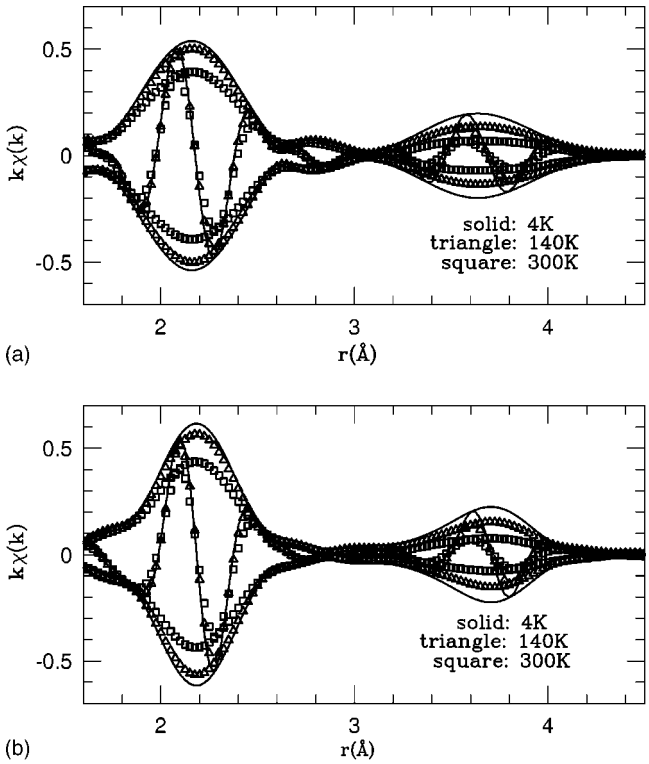

FIG. 8. (a) The Ga *K*-edge *r*-space data for $Sr_8Ga_{16}Ge_{30}$ at three different temperatures. (b) The Ge *K*-edge *r*-space data for the same sample.

A. Eu/Sr

Here we first describe the constraints for the Eu2 sites; the constraints for the Sr2 site are nearly identical. Neutron diffraction studies indicate a displacement of the Eu2 within the plane of the Eu2 cage (i.e., the *bc* plane in Fig. 1) with four off-center displacements (the 24*j* and 24*k* sites). The 24*j*-site, our $(0,\Delta,\Delta)$ model, assumes that the Eu2 is displaced equally along the $\pm\hat{b}$ and $\pm\hat{c}$ axes in the *bc* plane, toward the midpoint between two M2 sites. Our XAFS analysis indicates that this type of displacement agrees poorly with the data and therefore is not considered further here; we return to this result in the Discussion. A similar result was found in diffraction studies.[18,27] The second type of displacement used in diffraction studies (24*k*)—our $(0,0,\Delta)$ model—assumes that the Eu2 is displaced along either the $\pm\hat{b}$ or $\pm\hat{c}$ axis, toward a point just above or below the more distant M3 site (see Fig. 1).

However, the Eu2 cage does not have simple four-fold local symmetry but rather four-fold rotation-inversion symmetry about the *a*-axis if the Ga/Ge difference is ignored. (Since the Eu2-Ga and Eu2-Ge standards are very nearly identical we cannot differentiate various distributions of Ga on the different crystallographic sites.) Our third off-center displacement model retains the rotation-inversion symmetry—it is a displacement toward the most distant M3 site in the cage, i.e., a $\pm\hat{b}$ displacement Δ, plus a small component δ, in the $\pm\hat{a}$ directions (δ=0.154 Δ); we label this model $(\delta,\Delta,0)$. For this type of displacement the distances to the four equivalent nearest neighbors (M3 sites) are also equal. This is expected from local symmetry arguments, since if the nearest neighbors dominate the local potential, any minima will be at a point that is equidistant from them; consequently that is where the Eu2 most likely would be found. For this reason, it might be the more physically plausible model. This argument assumes the bonding to Ga and Ge are comparable; a significant difference in bonding strength, plus the nonuniform Ga/Ge distribution would change it.

Twenty pair-standards were used in the fit. Three represent Eu1-Ga/Ge pairs (one of which is the multiple scattering contribution), 15 represent Eu2-Ga/Ge pairs; again one is the sum of the small multiple scattering contributions. Another represents a composite peak for a possible on-center Eu atom contribution and the last represents the tails of the peaks at higher *r*, which have a small contribution within the fit range. Many constraints are needed to keep the number of parameters below the maximum possible number of degrees of freedom[33]—they are described below. All multiple scattering peaks are constrained such that the distances, amplitudes, etc. are consistent with the single scattering peaks.

The σ's are constrained according to the cage they are associated with. The two σ's for the Eu1 cage are set equal while the 16 for the Eu2 cage are separated into four different Eu2 subgroups as shown in Fig 9. The Eu2 groupings are motivated by the argument that the Eu2-Ga/Ge standards for the short bonds must have small σ's while those that contribute at high *r* should have large (static) σ's to account for the apparent disorder in the data between 3.5 and 4.4 Å (see Figs. 2 and 3).

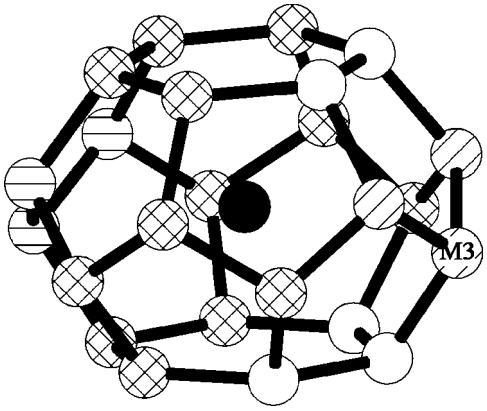

FIG. 9. σ groups for the fits: Closest neighbors (M3/M1)—white; second nearest neighbors (M2/M3)—diagonal lines; middle neighbors (M1/M2/M3)—crosshatch; distant neighbors (M2/M3)—horizontal lines.

The Eu1 positions are all constrained to their relative crystallographic proportions so that only the overall size of the Eu1 cage is allowed to vary. This maintains the cubic structure and imposes the constraint that Eu1/Sr1 is on-center.

As shown in Fig. 10 the Eu2 positions are more complex. Here, each line represents a Eu-cage-neighbor distance as a function of the Eu off-center displacement. In most cases the lines represent more than one atom pair, i.e., they are degenerate. Those lines that have a negative slope are associated with the Ga/Ge atoms on the side of the cage toward which the Eu2 is displaced; similarly, those that have a positive slope represent the Ga/Ge atoms on the opposite side of the cage. These two groups are referred to as "front of the cage" and "back of the cage," respectively. It should be noted that while the four nearest M3's are represented by two twofold degenerate lines in the $(0,0,\Delta)$ case, they collapse onto each other in the $(\delta,\Delta,0)$ case, i.e., when $\delta=0.154\ \Delta$.

In the fits the Eu2—Ga/Ge pair distances are constrained to correspond to a stiff Ga/Ge framework (see Sec. IV B where we show the variations of the Ga/Ge atomic positions are of order 0.03 Å) by applying the following argument. Assume there are two lines with slopes a and b (as in Fig. 10); then for small changes in the pair-distances Δr_i,

$$\Delta r_1 = a\Delta x, \tag{2}$$

$$\Delta r_2 = b\Delta x, \tag{3}$$

where Δx is the change in off-center displacement. Consequently,

$$\Delta r_2 = \Delta r_1 \frac{b}{a}. \tag{4}$$

If every line with negative slope is constrained to some "master" line (with slope a) then the positions of each of these Eu2 standards are crystallographically consistent with the closest half of the Eu2 cage being rigid and requires only one parameter to describe all the pair distances in the front of the cage. A similar set of constraints can be made for the back of the cage using a positive slope master line.

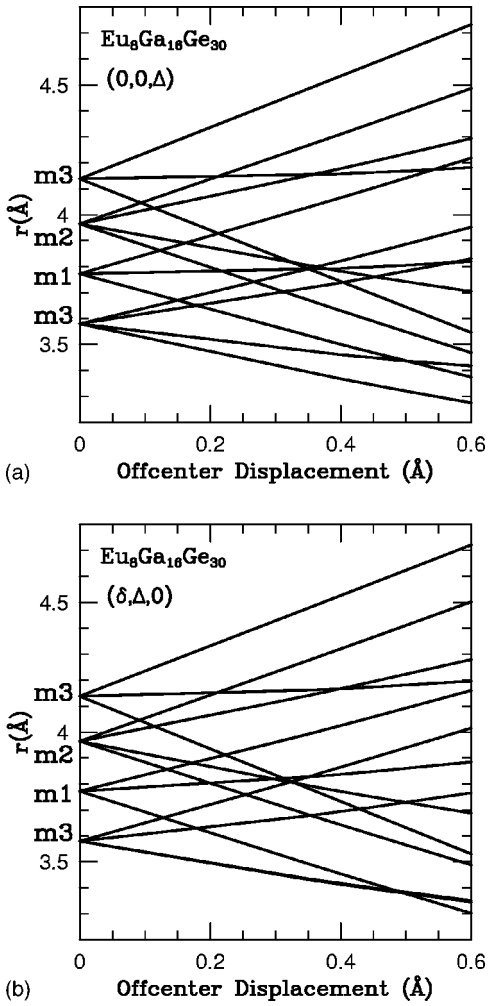

FIG. 10. The distances from Eu2 to its Ga/Ge neighbors as a function of the off-center displacement for the $(0,0,\Delta)$ and $(\delta,\Delta,0)$ models. The negative sloping line that has the smallest r-value at a displacement of 0.40 Å is the "master" line for the "front of the cage" group. The positive sloping line that has the smallest r-value at 0.40 Å is the "master" line for the "back of the cage" group.

Using these constraints, two types of fits were carried out: (1) the cage was assumed to be undistorted and one off-center distance was allowed, and (2) a front-back distortion of the cage was permitted by allowing slightly different off-center displacements for the front and back of the cage.

The amplitude of each standard is constrained to maintain the known number of Ga/Ge neighbor atoms at each pair distance, which are obtained from neutron diffraction. This constraint is imposed by setting the ratio of the amplitudes to be that required by the diffraction data. These fractional amplitudes are then multiplied by a constant S_o^2 to account for multielectron effects.

Since the overall E_o shift of the data should be constant, the E_o shifts for all the standards are constrained to be equal for all fits through the full temperature range. The value of E_o is determined at low temperatures where the XAFS signal has the best signal-to-noise ratio; an average value for E_o is obtained by averaging the results from fits of several scans at low T.

For fits with some of the Eu2 (or Sr2) assumed to be on center, the on-center Eu2 fraction is fixed and a single parameter σ is allowed to vary for this peak. The fraction is then varied in a series of fits.

The final component in the fit from 2.5 to 4.2 Å is a nonvariable standard that is a sum of the Eu1 and Eu2 peaks above the fit range. This is done by independently fitting the peak between 5.00 and 6.00 Å using a sum of the higher-r Eu1 and Eu2 peaks for each temperature. The results are then included as fixed contributions in the fits to the first multipeak to account for these small tails of the higher r peaks.

B. Ga/Ge

Fits were made for the Ga and Ge K-edge data for both samples. These fits are easier to set up because the main peaks at 2.491 and 3.970–4.001 Å are composed exclusively of on-center Ga/Ge-Ga/Ge standards. They include four standards for the Ga1/Ge1 site, four for the Ga2/Ge2 site, and five for the Ga3/Ge3 site. The σ's and displacements for each site are constrained within their own group. The amplitudes and E_o's are constrained by the methods outlined for the Eu and Sr fits. For these fits, the lattice is assumed to be composed exclusively of either Ga or Ge since their FEFF7 generated standards are almost identical for the peaks at 2.49 and 3.97–4.00 Å. Trial fits with a mixture of Ga-Ga and Ga-Ge standards did not make a significant difference for the Ga/Ge K-edge data; this is expected because the atomic number only changes by 1. EXAFS cannot differentiate between random or clustered distributions of Ga on the Ga/Ge sites.

V. FIT RESULTS

A. Eu

For the Eu data, the fits show that when a small fraction of on-center Eu2 is included, this component is broadened such that its peak-amplitude in r-space goes to ~ 0. For this reason, only fits that do not include an on-center Eu2 are presented. Figure 11 shows the excellent fits of the Eu data for the $(0,0,\Delta)$ and $(\delta,0,\Delta)$ models at 15 K. In these fits we have used ten free parameters with the constraints as described above. The differences between the fits to the two models are small and there is no significant variation in the goodness-of-fit parameter C^2 (proportional to the statistical χ^2 parameter). Therefore, from the perspective of a single trace, EXAFS is not sensitive enough to make a clear distinction between the models.

In these fits the Eu1-Ga/Ge distances agree within 0.01 Å with the average values from diffraction for a rigid Ga/Ge lattice and need no further discussion. The fit of the Eu1 site is very robust and is essentially unchanged for the various Eu2 off-center models. For the Eu2 site, the off-center distance is varied—plus a possible front/back distortion of the Ga/Ge cage. Figure 12 shows the Eu2 displacement as a function of T obtained from fits with a front/back cage distortion. The displacement Δ is nearly temperature independent and equal to 0.445 ± 0.020 Å for both models; $\delta = 0.07$ Å. A plot of displacement for the "back of the cage"

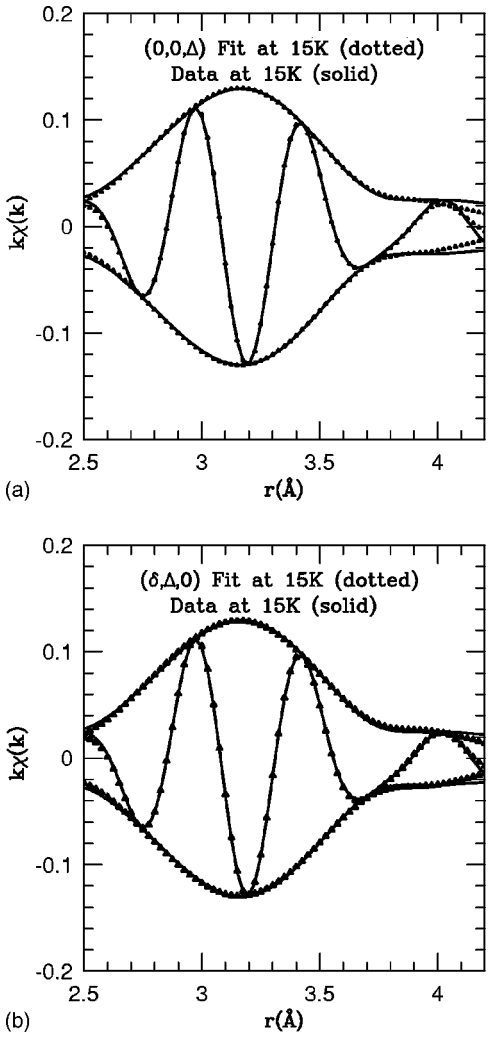

FIG. 11. Top: The excellent fit (dots) to the Eu data for the $(0,0,\Delta)$ model. Bottom: The corresponding fit of the Eu data for the $(\delta,\Delta,0)$ model. The fit range is 2.5–4.2 Å. The fits are indistinguishable except for a small variation between 4.1 and 4.2 Å.

atoms is not presented because the peaks they are associated with are strongly broadened and thus the off-center displacement for the "back of the cage" has a very large error ($\geqslant 0.10$ Å). Consequently, a comparable fit result can be obtained when no front/back distortion is allowed. This outcome reflects the fact that the Eu2-Ga/Ge pairs in the front of the cage are more highly ordered (a stronger bonding of Eu to the nearest cage atoms) and therefore dominate the observed XAFS signal for the Eu2 site. This is consistent with the theoretical calculations of Blake *et al.*[34] who note that (for the Sr case) the bonding to the nearest neighbors in the cage is strengthened (i.e., the Ga-Ge orbitals are stabilized) when the Sr moves off-center.

For understanding the rattling behavior of Eu in the Eu2 sites, the more important quantities are the σ_i^2 for each of the atom pairs [σ is the width of the pair distribution function (PDF)]. These parameters are plotted as a function of temperature in Fig. 13 for several atom pairs. Fits of these data to an Einstein model [Eq. (5) below] were carried out for each pair and the results are tabulated in Table II. Both the σ^2

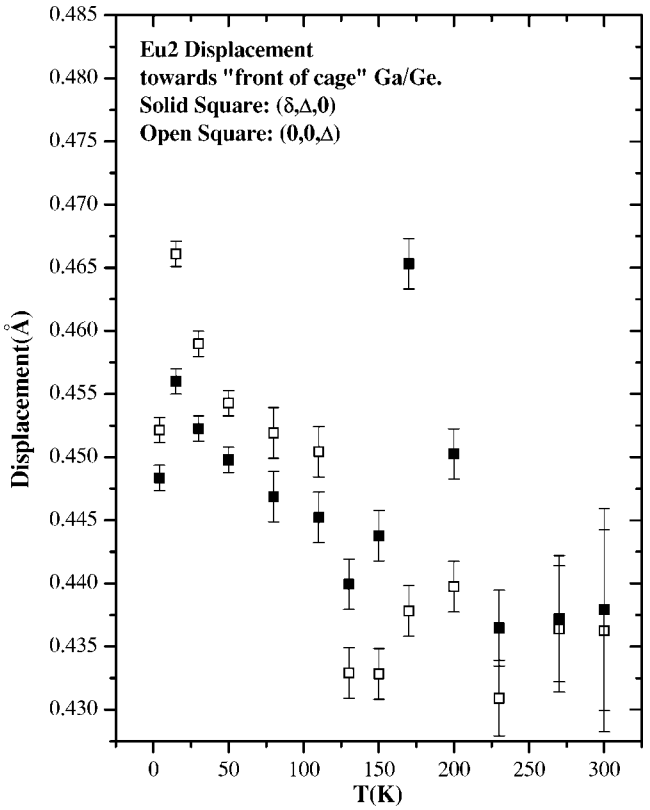

FIG. 12. The magnitude of the off-center displacement of Eu2 toward the "front of the cage" on an expanded vertical scale. Closed square: $(\delta,\Delta,0)$. Open square: $(0,0,\Delta)$.

vs T plots and the Einstein temperatures from the fits show that the vibration properties are similar for the two Eu2 off-center models.

The Einstein model assumes a single vibration mode frequency and is often used for optical phonons or local modes. For this model, σ_E^2 is given by

$$\sigma_E^2 = \frac{\hbar^2}{2M_R k_B \Theta_E} \coth \frac{\Theta_E}{2T}, \tag{5}$$

where M_R is the reduced mass, Θ_E is the Einstein temperature, and k_B is Boltzmann's constant. At high temperatures $(\Theta_E/T \leqslant 0.3)$, $\sigma_E^2(T) \propto T$.

In general there is also some static distortion. Then

$$\sigma^2 = \sigma_E^2 + \sigma_{static}^2. \tag{6}$$

For the $\sigma^2(T)$ fits, it is necessary to fix the Eu reduced mass M_R because the data are not good enough to yield a definite minima in C^2 when there are three free variables (M_R, θ_E, and σ_{static}^2). Since the Ga/Ge lattice is expected to be stiff relative to Eu vibrations, the Eu reduced mass is fixed at its atomic mass ($\sim$152 g/mol) while σ_{static}^2 and θ_E are allowed to vary.

As shown in Table II the fits for the Eu1 site [Fig. 13(a)] using the two different Eu2 off-center models yield $\theta_E \sim 78$ and $\sim$82 K. Note that σ_{static}^2 is a factor of 2 smaller for the $(\delta,\Delta,0)$ model than for the $(0,0,\Delta)$ model. Since the Eu1 site should have little to no static disorder, this result supports the $(\delta,\Delta,0)$ model. The C^2 parameters from the Einstein fits for the Eu1 site are also a factor of 2 smaller for the $(\delta,\Delta,0)$ model and provide further support for this model.

Table II also shows output parameters from fits of σ^2 vs T for the Eu2 "closest neighbor" group [see Fig. 13(b)]. These σ's are associated with the four nearest M3 site Ga/Ge atoms, toward which Eu2 is displaced; θ_E is $\sim$93 and $\sim$96 K for the two models. Note that for these neighbors, σ_{static}^2 is smaller for the $(0,0,\Delta)$ model than for the $(\delta,\Delta,0)$ model. This reflects the partial overlap between the Eu1-Ga/Ge peak and "closest neighbor" Eu2-Ga/Ge peak. Therefore it is unclear from the fits as to which site the static disorder belongs.

Fits to the Eu2 next nearest neighbors (near M2/M3)—not shown—are quite similar to those for the Eu2 "closest neighbor" site, though they have much larger errors as a result of the large scatter in σ^2. For both models, θ_E is $\sim$100 K. However, the rest of the Eu2 pair distribution functions are strongly disordered, $\sigma(T)$ for the remaining groups ("middle of cage" and "distant M2/M3") is large, $\sim$0.04 Å^2, and nearly independent of T. Since σ^2 is large even at low temperature, the broadening must be dominated by a large static component, including possible distortions of the cage because of variations in the Ga distributions, that obscures temperature dependent contributions. For this reason, no information about thermal vibrations can be extracted from these peaks. Because there is considerable static disorder for the longer pair distances in the Eu2 cage we argue that there is likely also some disorder for the closest neighbor PDF; consequently the larger static disorder for the closest neighbors for the $(\delta,\Delta,0)$ model described above is consistent with the other fits that support this model.

Finally, Einstein model fits for the Eu1 contribution to the peak between 5.00 and 6.00 Å [Fig. 13(c)] yields θ_E near 80 K, consistent with the nearest neighbor results. This is in fact a self-consistency check since $\sigma^2(T)$ for both the nearest neighbor and further neighbors about the Eu1 site will be dominated by the large amplitude vibrations of the Eu atom. For the Eu2 site contribution to this peak ($\sim$5 to 6 Å), $\sigma^2(T)$ is very large ($\sigma^2 \sim 0.04$ Å^2); consequently the amplitude of the Eu2 contribution is negligible compared to that for Eu1.

B. Sr

The first fits to the Sr data assumed only an off-center displacement for the Sr2 site. Figure 14 shows that this model cannot fit the data (at 15 K), particularly in the region between 3.4 and 3.8 Å where the phase in the real part of the transform fits poorly. No variation in the size of the Sr2 cage, or a front/back distortion of the cage, nor the difference between the various off-center models would fit in this region. In contrast, Fig. 15 shows the excellent fit for the $(\delta,\Delta,0)$ off-center model [fit to the $(0,0,\Delta)$ is similar] at 15 K when $\sim$25% of the Sr2 are on-center. The superiority of this fit is underlined by the fact that its C^2 parameter is 100 times lower than for the fit without an on-center component. For the fits that include an on-center component, it is difficult to find any difference between the two models in the EXAFS

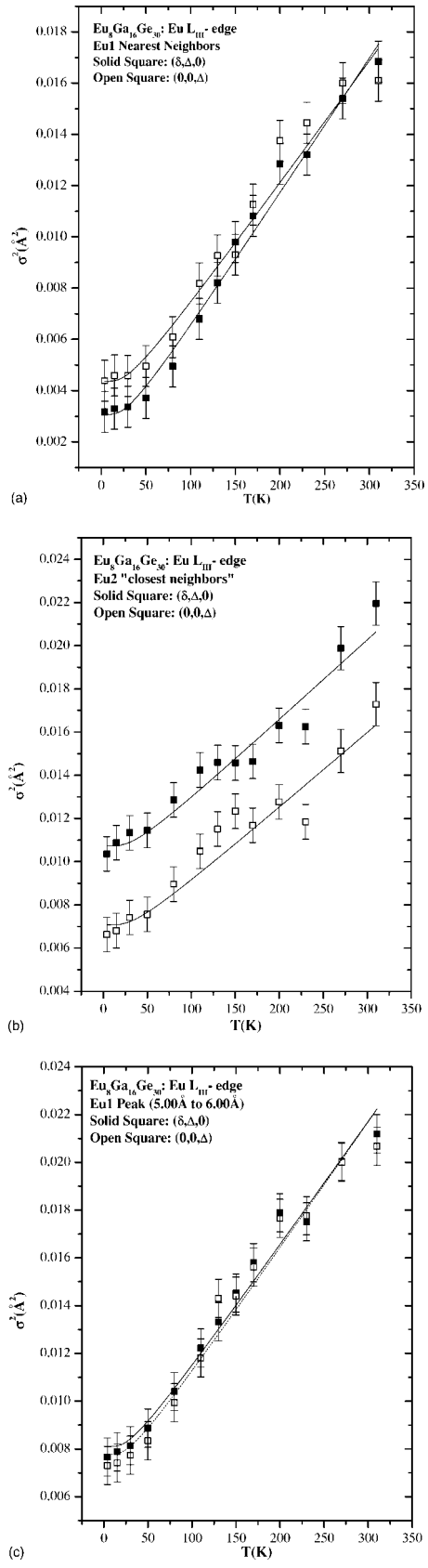

FIG. 13. (a) σ^2 vs T for the Eu1 site. (b) σ^2 vs T for the Eu2 "closest neighbors" site. (c) σ^2 vs T for the Eu "further neighbors" site.

TABLE II. Output parameters from fits to σ^2 vs T for the Eu1 and Eu2 sites assuming the Ga/Ge lattice is rigid and M_R for Eu is at its atomic mass (151.965 g/mol). C^2 is the goodness-of-fit parameter. S_o^2 is not precisely known; a change in S_o^2 shifts the plots in Fig. 13 up or down and mainly changes σ^2_{static}. For this reason, the errors given are relative errors; error for $\sigma^2_{static} \sim 0.001$ Å^2. The same S_o^2 is used for all fits so that the results for different models can be compared, i.e., $(0,0,\Delta)$ vs $(\delta,\Delta,0)$.

Site/Model	σ^2_{static}(Å^2)	θ_E(K)±10 K	$C^2(10^{-7})$
Eu1$(\delta,\Delta,0)$	0.0010	78	2.9
Eu1$(0,0,\Delta)$	0.0024	82	5.6
Eu2:closest$(\delta,\Delta,0)$	0.0090	93	6.1
Eu2:closest$(0,0,\Delta)$	0.0056	96	7.9

data. Visually they are identical and their C^2 parameters are comparable.

Figure 16 shows plots of the Sr off-center displacement Δ for the "front of the cage" for a fit where a front/back distortion is allowed. The displacement is nearly temperature independent and equal to 0.40±0.05 Å; δ=0.06 Å. A nearly identical result is obtained if no distortion is allowed, but with a larger error (±0.10 Å). Note that since only ~75% of the Sr2 are off-center, the average Sr2 displacement when the on-center fraction is included is ~0.30 Å in agreement with diffraction studies.[18,27]

σ^2 is plotted as a function of T for the various Sr -Ga/Ge pairs in Fig. 17. Einstein fits are made to $\sigma^2(T)$ using Eqs. (5) and (6); because of the stiffness of the Ga/Ge lattice, the reduced mass is again fixed at the rattler atomic mass (M_R for Sr ~87 g/mol), and σ^2_{static} and θ_E are allowed to vary (see Table III).

In the following discussion, the results are reported assuming that 25% of the Sr2 are on-center at all temperatures.

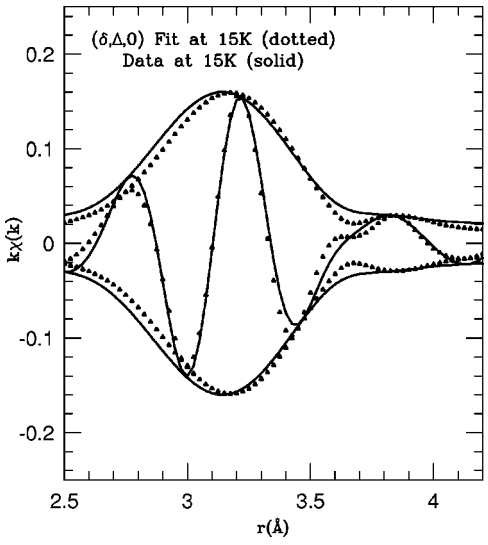

FIG. 14. The poor fit (dots) to the Sr data for the $(\delta,\Delta,0)$ model when no on-center Sr2 component is included. The main difficulty occurs near 3.5 Å where the phase of the fit does not fit the data; this r-range corresponds to the middle distances for the Sr2 site. The fit range is from 2.5 to 4.2 Å.

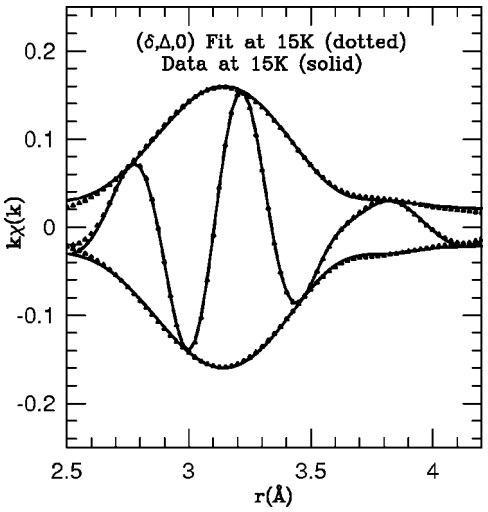

FIG. 15. Fit to the Sr data at 15 K for the $(\delta,\Delta,0)$ model. The fit include a 25% on-center Sr2 component; fit range is from 2.5 to 4.2 Å.

This is a rough approximation that requires some discussion. Fits show that the Sr2 on-center percentage appears to increase slightly between 15 and 200 K from 25±8% to 35±8%. This variation changes the Sr2 on-center σ but does not significantly affect any other parameters. When the on-center contribution is allowed to change with temperature, θ_E for the on-center Sr2 site drops to ~120±20 K, a ~30 K

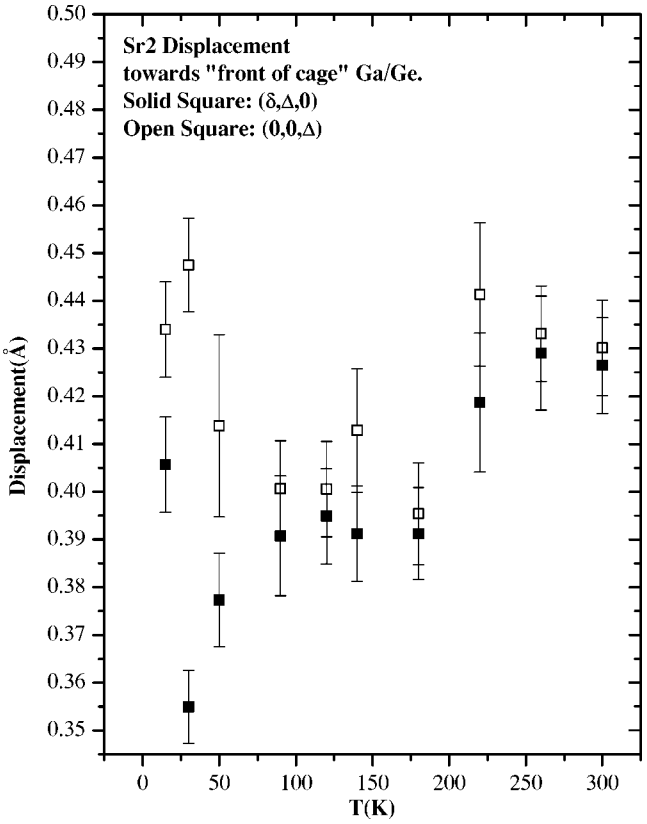

FIG. 16. Magnitude of the off-center displacement Δ of Sr2 toward the "front of the cage." Closed square: $(\delta,\Delta,0)$. Open square: $(0,0,\Delta)$ models. Note the small vertical scale.

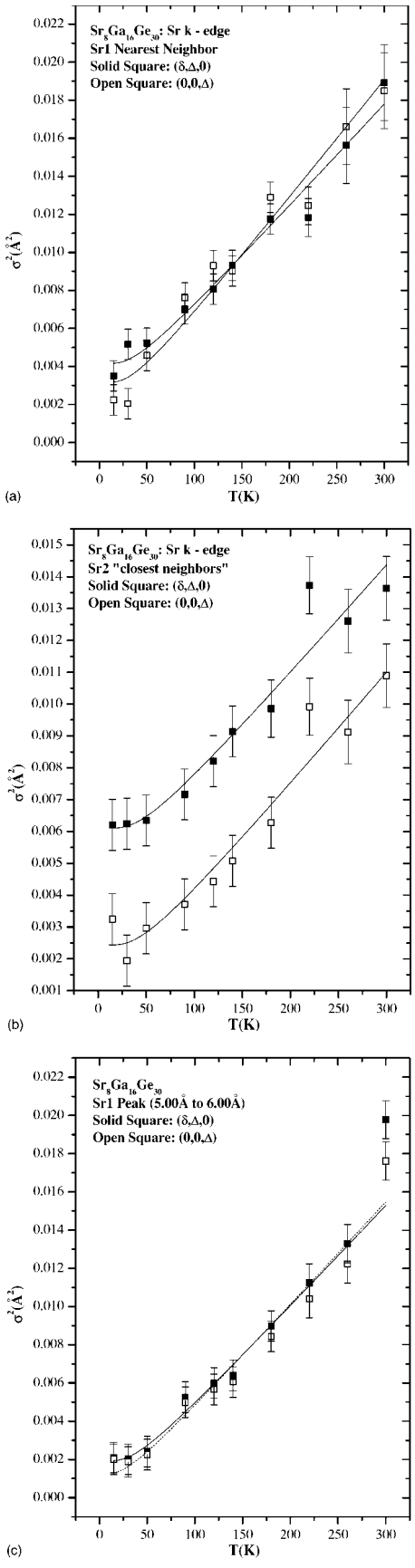

FIG. 17. σ^2 vs T for (a) the Sr1 site; (b) the Sr2 "closest neighbors" site; and (c) the Sr "further neighbors" site.

TABLE III. Output parameters from fits to σ^2 vs T for the Sr1 and Sr2 sites assuming the Ga/Ge lattice is rigid, M_R for Sr is near its atomic mass (87.62 g/mol), and 25% of the Sr2 are on-center.

Site/Model	σ^2_{static}(Å^2)	θ_E(K)±10 K	$C^2(10^{-7})$
Sr1$(\delta,\Delta,0)$	0.0014	102	6.9
Sr1$(0,0,\Delta)$	0.0002	95	13.7
Sr2 closest$(\delta,\Delta,0)$	0.0039	128	6.7
Sr2 closest$(0,0,\Delta)$	0.0002	126	6.0
Sr2 on-center$(\delta,\Delta,0)$	0.0041	156	4.0
Sr2 on-center$(0,0,\Delta)$	0.0031	147	3.8

decrease compared to the values in Table III; hence there is a large error for this θ_E because of the uncertainty in the on-center fraction.

As shown in Table III, θ_E for the Sr1 site is ~100 K for both models [Fig. 17(a)]; however, C^2 for the Sr1 site is considerably smaller for the $(\delta,\Delta,0)$ model than for the $(0,0,\Delta)$ model, which supports the $(\delta,\Delta,0)$ model, as found above for the Eu1 site. The static contribution σ^2_{static} is small for both models; because it is near the noise level (0.001 Å^2 at low T) it does not provide any differentiation between the models.

For the Sr2 "closest neighbor," θ_E is near 130 K [Table III and Fig. 17(b)]. Here, the C^2 parameters are comparable but σ^2_{static} is considerably larger for the $(\delta,\Delta,0)$ model as also found for the Eu2 site. Since the Sr2 site is expected to have a significant σ^2_{static} component based on the disorder in the Sr2 cage further neighbors, this again is more consistent with the $(\delta,\Delta,0)$ model.

σ^2 values for all the other Sr2 groups ("near M2/M3," "middle of cage," and "distant M2/M3") are uniformly large ($\sigma^2 \sim 0.025$); again the large static disorder at low temperature obscures any temperature dependent contributions. This is again consistent with calculations[34]—the Sr2-Ga/Ge bonds are strengthened for the short distances and weakened for the long bonds.

Finally the fit of $\sigma^2(T)$ for the Sr peak between 5.00 and 6.00 Å [Fig. 17(c)] yields θ_E near 100 K for the Sr1 site, again consistent with θ_E for the nearest neighbor peak. The contributions to this peak from Sr2 sites is small, as σ^2 is near 0.04 Å^2 for all temperatures.

C. Ga/Ge

Excellent fits to the first two shells of the Ga/Ge-Ga/Ge data were obtained and are shown in Fig. 18; these peaks occur near 2.2 and 3.6 Å (actual average distances 2.49 and ~4.0 Å); each is the sum of several closely spaced peaks. In addition, weak Ga/Ge-Eu/Sr peaks are also expected near 3.2 Å, but have a negligible amplitude. In these fits, C^2 is slightly better for the Ge edge fits than for the Ga edge fits. This reflects the poorer fit for the Ga data for the intermediate region between the main peaks (2.6–3.2 Å). Fits were also attempted using additional single Ga-Ga/Ge and Ga-Eu (Ga-Sr) peaks in this intermediate region. None of these additional peaks fit the data well in this region and gave unexpected (unphysical) atom-pair distances. More complex models involving several peaks were not considered. From these fits we have obtained $\sigma^2(T)$ for Ga and Ge in each sample, and the average bond distance of the neighbors about Ga and Ge.

Using Eqs. (5) and (6), fits of $\sigma^2(T)$ were made for the two main peaks (2.2 and 3.6 Å) for each sample. Since a pair of Ga/Ge-Ga/Ge atoms is expected to behave similarly to two equivalent masses connected by a stiff spring, M_R should be one-half the average atomic mass of Ga/Ge (69.72/72.61 g/mol). For the peak at 2.2 Å, C^2 indeed has a minima when M_R is one-half the Ga/Ge atomic mass. However, for the pair distribution at 3.6 Å, the error in σ^2 is too large to yield a clear C^2 minima. For this reason M_R is fixed at one-half the atomic mass for this further neighbor peak.

As shown in Table IV, θ_E for the peak at 2.2 Å is essentially the same for Ga and Ge in the two samples, ~311–314 K for Ga and ~322–326 K for Ge. For the Ga and Ge K-edge second neighbor peak at 3.6 Å, θ_E is also about the same, ~167–180 K for Ga and ~172–188 K for Ge. These values indicate that while the first neighbor Ga/Ge-Ga/Ge pairs are quite stiff, the second neighbors are much softer, suggesting the presence of bond angle disorder.

An interesting aspect is that the Ge edge data show considerably less static disorder for the Ge-Ga/Ge second neighbors at 3.6 Å than for the corresponding Ga-Ga/Ge neighbors from the Ga edge data. This effect is clear in Fig. 19(b) where σ^2_{Ga} is quite large at low T. Consequently, the bond angle disorder about the Ga atom must be much larger than around the Ge atom. To investigate this effect, fits were attempted using various distributions of Ga or Ge on the M1, M2, and M3 sites as suggested in a recent study.[22] In these fits, we used two standards to fit the second peak of the Ga K-edge data (a similar procedure was used for the Ge edge data). Unfortunately, C^2 for these fits was not significantly better than it was for a random distribution of Ga/Ge. However, the fits did suggest (with a large amount of error) that the Ge-Ga and Ga-Ge mixed-pair contributions are more disordered than the Ga-Ga or Ge-Ge pairs for the second neighbors.

Although the Einstein approximation fits the data fairly well, it makes more sense to use the correlated Debye model for the Ga/Ge lattice—this model describes the acoustic phonons at all possible k-vectors up to the Brillouin zone boundary (but also includes correlations in the local atomic vibrations). These are the phonons that should dominate the thermal behavior for the Ga/Ge framework with θ_{Debye} corresponding to the highest (longitudinal) acoustic phonon frequency in the crystal. Since EXAFS is primarily sensitive to radial vibrations it is less sensitive to the transverse modes.

As shown in Fig. 19(c), the Debye model fits very well (better than the fit with an Einstein model) θ_{Debye} is near 400 K for the nearest neighbor peak (2.2 Å) in the Ga K-edge data for $Sr_8Ga_{16}Ge_{30}$. Since plots of σ^2 vs T for the nearest neighbor peak (2.2 Å) for both samples and for both Ga and Ge edges are essentially identical within the errors [see Figs. 19(a) and 19(b)], all these peaks must also have θ_{Debye} near 400 K.

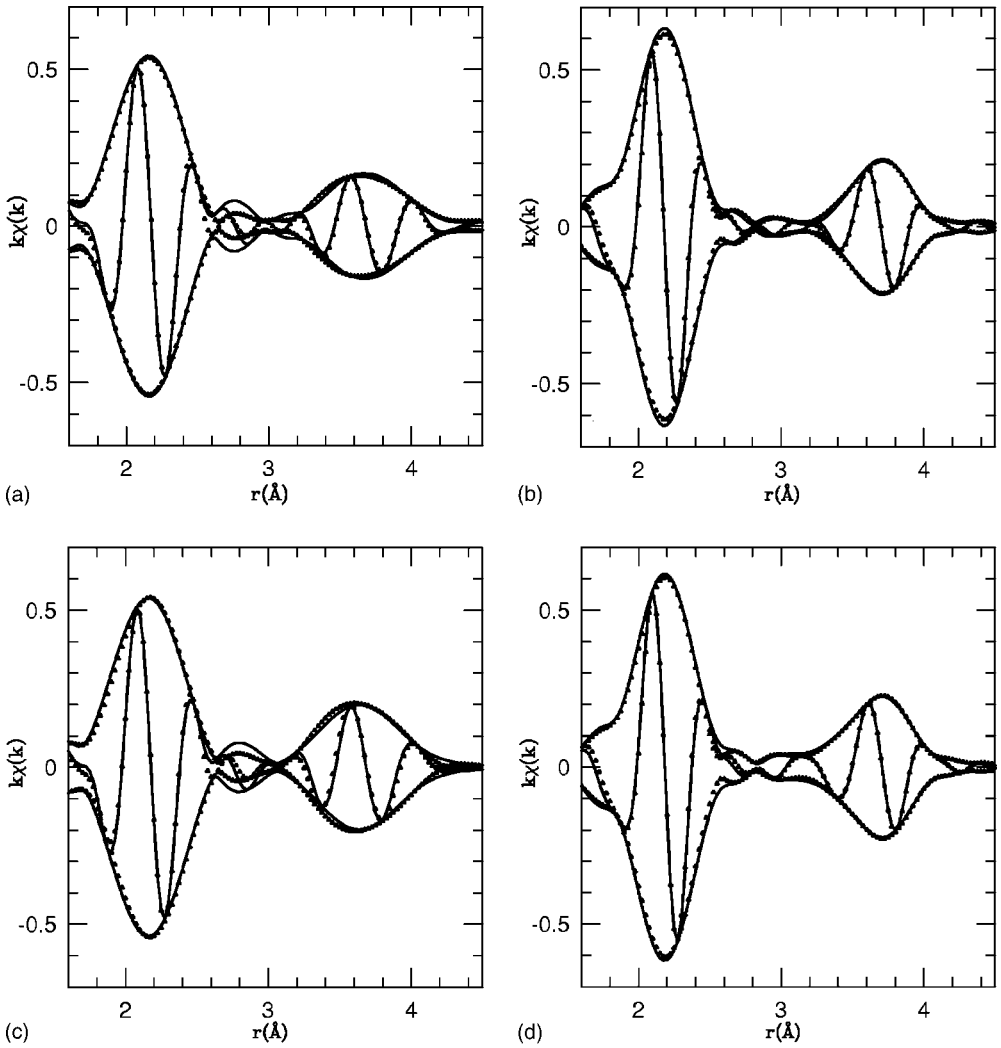

FIG. 18. Fits to: (a) the Ga *K*-edge data for $Eu_8Ga_{16}Ge_{30}$ at $T=4$ K; (b) The Ge *K*-edge data for $Eu_8Ga_{16}Ge_{30}$ at $T=4$ K; (c) the Ga *K*-edge data for $Sr_8Ga_{16}Ge_{30}$ at $T=4$ K; and (d) the Ge *K*-edge data for $Sr_8Ga_{16}Ge_{30}$ at $T=4$ K. In each case the solid line is the experimental data and the points are the fit. Note that the Ga data are fit over a *k*-range of 3.50–11.50 $Å^{-1}$ while the Ge data are fit over a *k*-range of 3.50–14.50 $Å^{-1}$. In these fits, a Ga/Ge-Sr2/Eu2 peak was not included.

The detailed fits also provide an independent estimate of the distortions in the Ga/Ge framework; they show that the Ga-Ga/Ge bonds are slightly longer than the Ge-Ga/Ge bonds at all temperatures, by about 0.03 Å. The results are the same for both Sr and Eu clathrates—the Ga-Ga/Ge bonds are slightly longer and the Ge-Ga/Ge slightly shorter

TABLE IV. Output parameters from fits to σ^2 vs T for the Ga/Ge-Ga/Ge neighbors at 2.2 and 3.6 Å for $Eu_8Ga_{16}Ge_{30}$ and $Sr_8Ga_{16}Ge_{30}$, where the Ga/Ge reduced mass is one-half the average atomic mass (34.9 and 36.3 g/mol). Errors on $\sigma^2_{static} \sim 0.0002$ $Å^2$.

Sample	Atom/Site	$\sigma^2_{static}(Å^2)$	$\theta_E(K) \pm 5$ K	$C^2(10^{-9})$
$Eu_8Ga_{16}Ge_{30}$	Ga/2.2 Å	0.0003	314	0.87
	Ga/3.6 Å	0.0035	167	88.09
	Ge/2.2 Å	0.0002	326	0.39
	Ge/3.6 Å	0.0003	172	78.77
$Sr_8Ga_{16}Ge_{30}$	Ga/2.2 Å	0.0002	311	0.02
	Ga/3.6 Å	0.0047	180	44.55
	Ge/2.2 Å	0.0003	322	0.27
	Ge/3.6 Å	0.0005	188	6.80

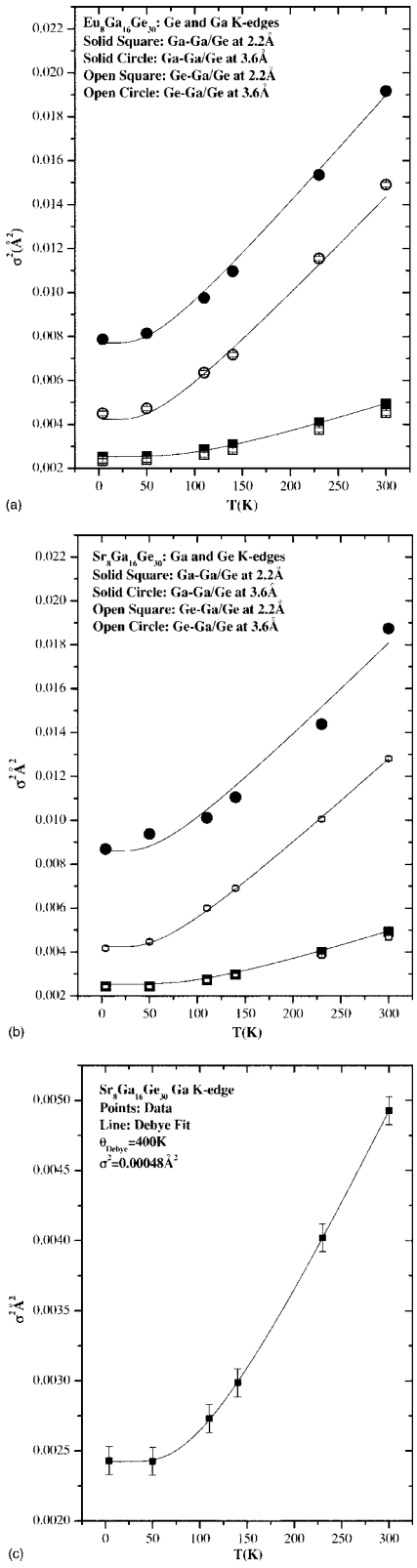

FIG. 19. (a) σ^2 vs T for the Ga/Ge nearest neighbor sites at 2.2 and 3.6 Å for $Eu_8Ga_{16}Ge_{30}$. (b) σ^2 vs T for the Ga/Ge nearest neighbor sites at 2.2 and 3.6 Å for $Sr_8Ga_{16}Ge_{30}$. Errors: ± 0.00012 Å^2 for first neighbors and ± 0.0007 Å^2 for second neighbors. (c) Debye fit to Ga K-edge data from $Sr_8Ga_{16}Ge_{30}$ for the Ga/Ge-Ga/Ge peak at 2.2 Å in the r-space data (actual bond length, 2.49 Å).

than the average value obtained in diffraction. From the fits to $\sigma^2(T)$ we find that the distribution of static distortions is also very small; $\sigma \sim 0.015$ Å for nearest neighbors and ~ 0.06 Å for the second peak (see Table IV). Thus the cage distortions up to the second neighbors are very small compared to the Eu and Sr off-center displacements.

VI. DISCUSSION

A. Eu/Sr rattlers

The low value of θ_E for the Eu1/Sr1 site (~ 80 K for Eu1 and ~ 100 K for Sr1) from EXAFS indicates that Eu1/Sr1 is loosely bound inside the cage and also acts like a rattler. In agreement with neutron diffraction results, the Eu1/Sr1 data can be modeled using no off-center displacement.[18,27] Additionally, since the Eu1 peak can be well modeled using only one σ for the two Eu1-Ga/Ge distances (see Fig. 18), the bonding must be comparable for each Eu1-Ga/Ge pair. Therefore the Eu1 vibrations are nearly isotropic—the same argument can be made for Sr1. The values found by EXAFS for θ_E are consistent with some recent Raman scattering results; for $Eu_8Ga_{16}Ge_{30}$ there is a Raman peak at 56 cm^{-1}(81 K) which compares well with $\theta_{E(\mathrm{Eu1})} \sim 80$ K. For $Sr_8Ga_{16}Ge_{30}$ the Raman peak at 65 cm^{-1}(94 K) is close to $\theta_{E(\mathrm{Sr1})} = 100$ K.[35]

The interaction between Eu2 (or Sr2) and the cage is more complex. In agreement with neutron diffraction results, the Eu2 and most of the Sr2 are off-center approximately along the $\pm\hat{b}$ or $\pm\hat{c}$ axes;[18,22,27] specifically, the EXAFS results indicate that the Eu2/Sr2 atoms are not displaced towards the M2 site Ga/Ge atoms. The EXAFS results also suggest that the off-center Eu2/Sr2 likely has a small displacement along the $\pm\hat{a}$ axis to make the distance to the four nearest neighbors M3 sites equal. The magnitude of the $\hat{a}$ displacement (0.06 to 0.07 Å) is within the thermal distribution found in neutron diffraction studies.[18,27]

Additionally, the different Eu2/Sr2-Ga/Ge pairs in the site 2 cage have distinctly different thermal behavior as evidenced in the σ^2 vs T plots. This variation in σ^2 with r for the Eu2 and Sr2 sites can be seen in the raw EXAFS data as illustrated in Fig. 20, where the Eu1 or Sr1 contributions have been subtracted from the original data at 15 K; for the Sr K-edge, the on-center Sr2 contribution has also been subtracted. Here the Eu2/Sr2 experimental results are compared with a uniformly broadened Eu2 or Sr2 peak ($\sigma = 0.10$ Å), calculated (FEFF7) using off-center displacements of 0.45 and 0.35 Å for Eu2 and Sr2, respectively.

This comparison emphasizes the changing disorder within the Eu2/Sr2 cage as r increases. Ordered pairs (small σ, large amplitude) occur at low r while disordered pairs (large σ, small amplitude) appear at high r. Since a small σ represents positively correlated motion[36] between a Eu2/Sr2-Ga/Ge pair (i.e., the Eu2 and Ga/Ge pairs move in the same direction), this picture emphasizes the fact that both Eu2 and Sr2 are bonded to the "closest neighbors" in the cage, the M3 sites, consistent with theoretical calculations. Fits of $\sigma^2(T)$ to an Einstein model yield θ_E values of ~ 95 and ~ 125 K for $Eu_8Ga_{16}Ge_{30}$ and $Sr_8Ga_{16}Ge_{30}$. These values

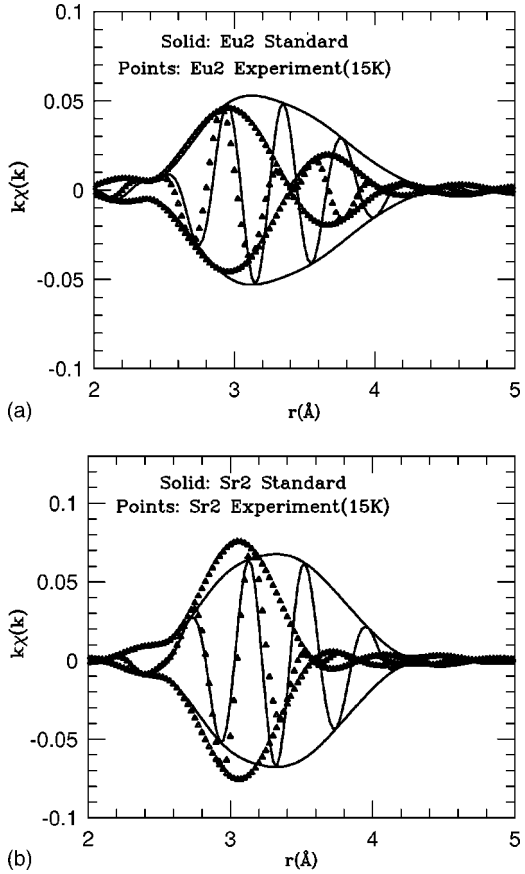

FIG. 20. (a) The Eu2 standard vs the Eu2 fit. (b) The Sr2 standard vs the Sr2 fit.

compare quite well with the Raman spectroscopy peaks found at 69 cm^{-1}(101 K) and 86 cm^{-1}(125 K) for $Eu_8Ga_{16}Ge_{30}$ and $Sr_8Ga_{16}Ge_{30}$, respectively.[9]

In contrast, the large $\sigma^2(T)$ for the more distant neighbors in the cage, particularly at low temperatures, indicates that the static disorder for these pairs is very large. Therefore there must be very weak bonding between Eu2/Sr2 and these more distant Ga/Ge neighbors in the cage. The first shell XAFS *r*-space data is sensitive primarily to radial motions of neighbors; vibrations of the rattler that are nearly perpendicular to the nearest neighbor bonds might well have lower Einstein temperatures [such as the low frequency modes found in Raman scattering studies at 23 cm^{-1}(33 K) and 32 cm^{-1}(46 K) for $Eu_8Ga_{16}Ge_{30}$ and $Sr_8Ga_{16}Ge_{30}$, respectively[9]] but are masked in the EXAFS data by the large amount of static disorder for the more distant Ga/Ge neighbors in the Eu2/Sr2 cage.

The behavior of $\sigma^2(T)$ for the other Eu2/Sr2-Ga/Ge groups is different for the Eu and Sr compounds. For the Eu2 site, the PDF for the second nearest neighbors (mixture of M2/M3 sitres) has a well-defined σ^2 vs T plot that yields a θ_E comparable to that for the "closest neighbors." In contrast, the "M2/M3" Sr2-Ga/Ge pair distribution has a σ^2 that is uniformly large and similar to the "middle of cage" and "distant M2/M3" Eu2/Sr2-Ga/Ge pair distributions. Consequently the Eu is bonded to a few more neighbors on the end of the cage and the off-center displacement may be more stable.

This raises the question as to why they might be different; one way to address it is to consider the atomic radii (ionic and covalent) of Eu, Sr, Ga, and Ge. The covalent radii of Ga and Ge are 1.22 and 1.26 Å, respectively. Consequently, a cage that is rich in Ga would be slightly smaller. The ionic radius of Eu is also nearly the same as that of Sr (but in lower coordinated sites);[22] however, the difference in radii is much larger for empirical radii[37] [Eu−1.86 Å, Sr−2.0 Å] which might be the reason all the Eu is off-center with a slightly larger off-center displacement. Note that the shortest Eu2-Ga/Ge and Sr2-Ga/Ge bonds (about 3.4 Å) are much too long to be simple covalent or highly ionic bonds; the empirical atomic radii give a more comparable bond length, but are still short by 0.1–0.3 Å. Varying amounts of ionicity/covalency and the large coordination number may be important factors.

Another possibility is that the potential for Sr2 is very close to the crossover point from off-center to on-center behavior as observed earlier for Ag^+ ions in RbCl (Ref. 38) and KI.[39] Near the crossover point a system becomes very sensitive to pressure—tiny strains can move the system from off-center to on-center. Because there is some disorder in the cage around the Sr atom, the local strains might be the determining factor as to whether a particular Sr2 atom is on- or off-center.

However, the most crucial aspect likely concerns the nature of the bonding between the rattler atom and the site 2 cage. This in turn depends on several properties of these systems—some of which have not yet been discussed in detail. (1) What is the distribution of Ga on the Ge sites? Is it sample dependent? (2) What is the net charge on the Ga, are they (slightly) negatively charged? (3) Does the possibility of an off-center displacement in site 2 depend on local variations in the stoichiometry?

Point (1) has been partially addressed for a few samples. Although there is relatively little scattering contrast between Ga and Ge both for x rays and neutrons, anomolous (resonant) scattering near an absorption edge (here the Ga and Ge edges) can provide such contrast. Zhang *et al.*[22] used this technique to examine the Ga distribution in a $Sr_8Ga_{16}Ge_{30}$ (and also a mixed Sr/Eu sample). In the Sr sample (likely *n*-type although not reported) they find a preference for Ga occupation on the 6*c* site (M1) (76% Ga, 24% Ge) and a low (essentially reversed) occupation of the 16*i* site (M2) (24% Ga, 76% Ge). The more plentiful 24*k* site (M3) has 43% Ga, 57% Ge. Based on these percentages, there are more Ga atoms in the 24-atom site 2 cage than in the site 1 cage, and the site 2 distribution of Ga is as follows: 3 Ga (out of 4) on the M1 site, 1.9 Ga (out of 8) on the M2 site, 3.44 Ga (out of 8) on the closest M3 site, and 1.72 Ga (out of 4) on the more distant M3 site. The theoretical calculations of Gatti *et al.*[13] support this general trend, although they did not make calculations for a wide range of Ga distributions.

Let us assume for now that this distribution is similar for many of the clathrates. Then the EXAFS (and diffraction) result, that the Eu and Sr are off-center towards the 24*k* positions and not the 24*j* positions, i.e., towards the nearest neighbor M3 sites and not the M2 sites, would suggest that the Eu2 and Sr2 atoms do not bind to the Ge (M2) sites, but rather to the nearest neighbor M3/M1 sites (see nearest

neighbors in Fig. 9) which have a high fraction of Ga. Since recent calculations indicate that the interaction between the rattler atom and the site 2 cage is ionic, this suggests that point (2) above may be correct, that the Ga is negatively charged. This argument is clearly not definitive but points out the need to know whether the ionic bonding discussed by Gatti *et al.*[13] requires the Ga atoms to be negative, and of course, whether this experimental Ga distribution is representative of many systems. A further complication is whether or not the Ga are uniformly distributed on the M3 sites—if there is a strong ionic attraction between the rattler and Ga atoms then the Ga atoms might be clustered on a subset of M3 sites close to the off-center atom (in the the extreme case there might be only one off-center direction). This clearly will change with the strength of the interactions and hence to the type of rattler. Clearly new experiments and further calculations are needed on a range of samples.

Finally we note that if the interaction between the rattler atom and the site 2 cage is via the Ga atoms, then the number of Ga atoms in a particular cage will be very important, and the off-center displacement within the site 2 cage for some rattlers may depend on the number of Ga present, point (3) above (and hence on whether the system is *n*-type or *p*-type). The EXAFS result, that some of the Sr2 appear to be on-center, might then be explained by a variation in stoichiometry in the sample.

B. Ga/Ge framework

The first neighbors in the Ga/Ge lattice are modeled using the Debye model with $\theta_{\mathrm{Debye}} \sim 400$ K for the acoustic phonons. These are the phonons that should dominate the thermal behavior for the Ga/Ge framework. It is not surprising that θ_{Debye} in EXAFS is comparable to (slightly larger than) the highest Raman mode observed at 260 cm^{-1}(377 K).

The second peak is more disordered. θ_E for this peak is ~176 K for both the Eu and Sr samples. Since it is clear that there can be very little variation in the first neighbor bonding, this result indicates that there is some fluctuation of the bond angle between Ga/Ge-Ga/Ge second neighbors. In addition, there is greater static disorder for the Ga edge data than for the Ge edge data. Since the lattice has approximately twice as many Ge as Ga, this result possibly suggests that the larger number of mixed linkages (i.e., Ga-Ge-Ge or Ga-Ge-Ga) for the Ga edge may be the reason for the larger bond bending disorder.

C. Implications for thermal conductivity

One of the novel characteristics of the Eu and Sr clathrates is their very low, glasslike thermal conductivity which makes them attractive candidates for potential thermoelectric applications. In contrast, the *n*-type Ba material has a significantly higher lattice conductivity overall and a peak at low temperature, more typical of crystalline materials. However, very recent thermal conductivity measurements[19] on *p*-type $Ba_8Ga_{16}Ge_{30}$ are more similar to $Sr_8Ga_{16}Ge_{30}$ and have a dip/plateau region near 20 K suggestive of a strong increase between the coupling of the Ba rattler and the lattice. Although Bentien *et al.*[19] suggest that this is primarily the result of phonon-electron/hole coupling, it could also be explained by an increased coupling due to stronger Ba-Ga/Ge bonds if the Ba is off-center in the *p*-type material, but on-center in *n*-type material. It is therefore crucial that structural data be obtained for a range of Ba (and other) clathrates with different carrier concentrations, from *n*- to *p*-type.

The off-center displacement of a rattler in the site 2 cage is the result of stronger bonds between the rattler and a few atoms in the cage, as compared to the weaker, longer bonds (to more or all of the cage neighbors) when the rattler is on-center. The EXAFS results confirm these stronger bonds for Sr2 (Eu2) as do theoretical calculations.[34] Here we note (neglecting for the moment the rattling motion) that if a rattler atom is bonded to the side of the cage it produces a large symmetry-breaking mass defect which should scatter phonons very efficiently; in contrast an on-center atom does not break the symmetry and would not scatter phonons (a small distortion of the on-center position arising from defects, etc., will produce a weak scattering and is included in Rayleigh scattering). This leads to a contribution to $\kappa(T)$ that has a linear T dependence at low T. In addition, the stronger bonds to a few atoms for the off-center case increases the coupling between the rattler vibrations and the framework phonons, and hence increases the resonant scattering contribution when the rattler is off-center.[40]

Several mechanisms have now been suggested to explain the low T dependence of the lattice thermal conductivity in the clathrates; (1) tunneling[41] which probably is only important at very low T, and (2) a varying phonon/charge-carrier scattering[19] that may be sample dependent, and the symmetry breaking off-center mass defect (plus enhanced phonon-rattler coupling) for off-center atoms described briefly above.[40] Because of the large variation in the thermal conductivity from sample to sample, that has been observed recently, detailed structural and transport measurements on the same material for a range of sample preparations will be needed to understand the rather complex low T behavior for $\kappa(T)$.

VII. CONCLUSIONS

The Ga/Ge network forms a relatively rigid lattice—the correlated Debye temperature for the nearest neighbor bonds is ~400 K indicating stiff bonds; it is the same for both Ga and Ge atoms, and for both samples. This value is primarily a measure of the longitudinal vibration modes and is comparable to the highest Raman modes observed in these systems. It is larger than the average θ_D obtained when a measurement averages over both acoustic and transverse modes such as the heat capacity (~300 K[10]) and the isotropic U parameters (271 K[18]). The main disorder within the cages of this lattice can be inferred from the broadening of the second neighbor Ga-Ga/Ge (or Ge-Ga/Ge) PDF; this peak has considerable disorder—and when combined with the stiff nearest neighbor bonds indicates bond-bending disorder. The broadening of this PDF for the Ga *K*-edge data is particularly large at low T, indicating that much of the static bond-bending disorder is related to the Ga atoms.

The filler atoms Sr and Eu in these *n*-type materials are located inside the two cages (sites 1 and 2). In both sites they are loosely bound and have large amplitude radial vibrations at quite low temperatures ($\theta_E \sim 80$ and 100 K for Eu1 and Sr1; 95 and 125 K for the *shortest* Eu2 and Sr2 bonds). Vibrations transverse to the bond (for Eu2/Sr2) are not easily observed but likely would lead to still lower values for θ_E as observed in diffraction. Consequently Sr and Eu atoms on both sites form rattler atoms which can scatter phonons effectively. The EXAFS results show that Eu is off-center, approximately 0.45 Å, in agreement with earlier diffraction results; however, the overall results suggest that the displacement is not just in the $\hat{b}\hat{c}$ plane but also may have a small component along the $\hat{a}$ axis [our $(\delta,\Delta,0)$, model]—this displacement has the four-fold rotation-inversion symmetry of the site 2 cage, but this would change if there is Ga clustering on the M3 site.

For the Sr, the fit of the EXAFS data is poor unless a fraction ($\sim$25%) of the Sr are on-center. Then the off-center displacement is about 0.4 Å; however, the average displacement over all Sr is 0.3 Å, in good agreement with the diffraction results. Again the overall results are better with the $(\delta,\Delta,0)$ off-center displacement model.

An important result from the EXAFS analysis is that the broadening of the Eu2-Ga/Ge or Sr2-Ga/Ge pair distribution functions is not uniform—the PDF for the shortest bond to the cage has a fairly small static disorder and a typical temperature dependence for $\sigma^2(T)$, described well using an Einstein model. In contrast the PDF's for the more distant Eu2-Ga/Ge or Sr2-Ga/Ge pairs have a large static disorder and little T dependence. This indicates that the Eu2 or (off-center) Sr2 atoms are bonded to the side of the cage, and hence are more strongly coupled to a few cage atoms than for an on-center position. This bonding also adds a mass defect on the side of the cage for the off-center case; it is randomly distributed over the four possible off-center sites.

The bonding to the side of the cage has very important consequences for the thermal conductivity. Since the off-center atoms are more strongly coupled to a few cage atoms they will have a larger effect in scattering phonons than on-center atoms. This needs to be included in understanding the large differences observed for the thermal conductivities of the Ba, Sr, and Eu clathrates.

Several questions remain while many new questions have been raised, in part by more detailed calculations, but also by the unexpected variation of the lattice thermal conductivity from sample to sample that has been observed recently. What are the tunneling splittings of the off-center Eu2 and Sr2 atoms and how broad is the distribution of such states for various types of samples? Within the Zintl concept the Ga atoms would be negative—is there any net negative charge on these atoms and does it significantly affect the interaction between the rattler atom and the site 2 cage? What aspects determine why the rattler atom moves off-center, and is it possible for some rattlers to shift from an on-center position to an off-center displacement with changes in the stoichiometry, or changes in homogeneity? Can smaller atoms form off-center rattlers in the smaller, site 1 cage? More generally, can other thermoelectric materials—such as the skutterudites—be prepared with off-center rattler atoms? (We have shown that for many of the filled Sb skutterudites, the rattler is in fact on-center.)[16] These and other questions must be answered before we can begin to optimize the properties of these materials for thermoelectric applications.

ACKNOWLEDGMENTS

The work at UCSC was supported by NSF Grant No. DMR0071863. The experiments were performed at SSRL, which is operated by the DOE, Division of Chemical Sciences, and by the NIH, Biomedical Resource Technology Program, Division of Research Resources.

[1] J. Dong, O. F. Sankey, and C. W. Meyers, Phys. Rev. Lett. **86**, 2361 (2001).
[2] G. S. Nolas and G. A. Slack, Am. Sci. **89**, 136 (2001).
[3] B. Iversen, A. Palmqvist, D. Cox, G. Nolas, G. Stuckey, N. Blake, and H. Metiu, J. Solid State Chem. **149**, 455 (2000).
[4] G. A. Slack, in *CRC Handbook of Thermoelectrics*, edited by D. M. Rowe (Chemical Rubber, Boca Raton, FL, 1995), p. 407.
[5] D. J. Brown and W. Jeitschko, J. Less-Common Met. **76**, 33 (1980).
[6] N. T. Stetson, S. M. Kauzlarich, and H. Hope, J. Solid State Chem. **91**, 140 (1991).
[7] C. B. H. Evers, L. Boonk, and W. Jeitschko, Z. Anorg. Allg. Chem. **620**, 1028 (1994).
[8] M. E. Danebrock, C. B. H. Evers, and W. Jeitschko, J. Phys. Chem. Solids **57**, 381 (1996).
[9] G. S. Nolas, T. Weakley, J. Cohn, and R. Sharma, Phys. Rev. B **61**, 3845 (2000).
[10] B. C. Sales, B. Chakoumakos, R. Jin, J. Thompson, and D. Mandrus, Phys. Rev. B **63**, 245113 (2001).
[11] N. P. Blake, L. Mollnitz, G. Kresse, and H. Metiu, J. Chem. Phys. **111**, 3133 (1999).
[12] A. Bentien, A. E. C. Palmqvist, J. D. Bryan, S. Latturner, G. D. Stucky, L. Furenlid, and B. B. Iversen, Angew. Chem., Int. Ed. **39**, 3613 (2000).
[13] C. Gatti, L. Bertini, N. P. Blake, and B. B. Iversen, Chem.-Eur. J. **9**, 4556 (2003).
[14] D. Cao, F. Bridges, S. Bushart, E. D. Bauer, and M. B. Maple, Phys. Rev. B **67**, 180511(R) (2003).
[15] E. D. Bauer, A. Slebarski, N. Frederick, W. Yuhasz, M. Maple, D. Cao, F. Bridges, G. Giester, and P. Rogl, J. Phys.: Condens. Matter **16**, 5095 (2004).
[16] D. Cao, F. Bridges, P. Chesler, S. Bushart, E. D. Bauer, and M. B. Maple, Phys. Rev. B **70**, 094109 (2004).
[17] D. Cao, F. Bridges, P. Chesler, E. D. Bauer, and M. B. Maple (unpublished).
[18] B. Chakoumakos, B. Sales, and D. Mandrus, J. Alloys Compd. **322**, 127 (2001).
[19] A. Bentien, M. Christensen, J. D. Bryan, A. Sanchez, S. Paschen,

F. Steglich, G. D. Stucky, and B. B. Iversen, Phys. Rev. B **69**, 045107 (2004).
[20] C. Uher, J. H. Yang, and S. Q. Hu, Mater. Res. Soc. Symp. Proc. **545**, 247 (1999).
[21] G. S. Nolas, J. L. Cohn, G. A. Slack, and S. B. Schujman, Appl. Phys. Lett. **73**, 178 (1998).
[22] Y. Zhang, P. L. Lee, G. S. Nolas, and A. P. Wilkinson, Appl. Phys. Lett. **80**, 2931 (2002).
[23] F. Bridges, R. Baumbach, D. Cao, P. Chesler, M. Anderson, and B. Sales, Radiat. Eff. Defects Solids **158**, 343 (2003).
[24] V. Narayanamurti and R. O. Pohl, Rev. Mod. Phys. **42**, 201 (1970).
[25] F. Bridges, CRC Crit. Rev. Solid State Sci. **5**, 1 (1975).
[26] R. P. Hermann, F. Grandjean, P. Bonville, H. Grimm, W. Schweika, G. Nolas, and G. J. Long, Bull. Am. Phys. Soc. **49**, 526 (2004).
[27] B. Chakoumakos, B. Sales, D. Mandrus, and G. S. Nolas, J. Alloys Compd. **296**, 80 (2000).
[28] J. J. Rehr, C. H. Booth, F. Bridges, and S. I. Zabinsky, Phys. Rev. B **49**, 12347 (1994).
[29] T. M. Hayes and J. B. Boyce, in *Solid State Physics* (Academic, New York, 1982), Vol. 37, p. 173.
[30] G. G. Li, F. Bridges, and C. H. Booth, Phys. Rev. B **52**, 6332 (1995).
[31] See http://lise.lbl.gov/RSPAK.
[32] S. I. Zabinsky, J. J. Rehr, A. Ankudinov, R. C. Albers, and M. J. Eller, Phys. Rev. B **52**, 2995 (1995).
[33] E. A. Stern, Phys. Rev. B **48**, 9825 (1993).
[34] N. P. Blake, S. Latturner, J. D. Bryan, G. D. Stucky, and H. Metiu, J. Chem. Phys. **115**, 8060 (2001).
[35] G. Nolas and C. Kendziora, Phys. Rev. B **62**, 7157 (2000).
[36] C. H. Booth, F. Bridges, E. D. Bauer, G. G. Li, J. B. Boyce, T. Claeson, C. H. Chu, and Q. Xiong, Phys. Rev. B **52**, R15745 (1995).
[37] See website http://www.webelements.com, for various ionic and empirical radii.
[38] F. Bridges and M. Jost, Phys. Rev. B **38**, 12105 (1988).
[39] A. Sievers and L. Greene, Phys. Rev. Lett. **52**, 1234 (1984).
[40] F. Bridges and L. Downward, Phys. Rev. B **70**, 140201(R) (2004).
[41] J. L. Cohn, G. S. Nolas, V. Fessatidas, T. H. Metcalf, and G. A. Slack, Phys. Rev. Lett. **82**, 779 (1999).